TURUN YLIOPISTO
Matemaattis-luonnontieteellinen tiedekunta

Migmatite textures from Kilpisjärvi region

Veeti Nurmi

Geology (Bedrock geology)
Master's thesis
Credits: 30 ECTS

27.2.2026
Turku

Pro gradu -tutkielma

Pääaine: Kallioperägeologia
Tekijä: Veeti Nurmi
Otsikko: Migmatite textures from Kilpisjärvi region
Ohjaajat: Esa Heilimo, Jaana Halla
Sivumäärä: 54 sivua + liitteet 2 sivua
Päivämäärä: 27.2.2026

Migmatiitit ovat keski- tai korkean asteen metamorfisia kiviä, joissa on kaksi tai useampi eroavaa osaa. Ainakin yksi näistä osista on syntynyt sulamistuotteena ja on yleisesti vaaleampi väriltään. Migmatiittien osat esiintyvät kivessä eri tavoin riippuen sulan määrästä ja vallinneesta paineesta. Kilpisjärven alueen geologia on laajalti tuntematonta arkeeista kiviainesta. Arkeeisen materiaalin lisäksi alueen luoteisosasta löytyy Kaledonidien aikaista geologiaa. Laassaniemen ja Kilpisjärven alueen geologista tietämystä voidaan parantaa tutkimalla paikallisia migmatiittirakenteita ja niiden yhteyksiä muuhun alueen geologiaan.

Tässä tutkielmassa migmatiittien tutkimiseen käytettiin valokuvia ja arkeeisia näytekiviä Laassaniemen alueelta, Kilpisjärveltä. Alueen näytekivistä tehtiin myös ohuthieitä, joita tutkittiin mikroskoopilla. Kilpisjärven migmatiittien sulan määrä vaihtelee sulamattomasta amfiboliitista täysin sulaneisiin leukosomirakenteisiin, jossa ei ole alkuperäisiä rakenteita havaittavissa. Alueen rakenteiden avulla on mahdollista selvittää sulan kulkusuunta ja koostumus. Ohuthienäytteistä pystyy tulkitsemaan mikroskopisia sularakenteita ja kiven eheyttä. Vaikka ohuthienäytteiden mineralogia on lähes samanlainen näytteissä, näytteiden tekstuurilliset vaihtelut ovat huomattavia ja tuovat tärkeää tietoa sulan liikkeistä. Vaikka metateksiitti-diateksiitti-vaihettumisvyöhykkeen suuruus ei ole tiedossa, se voi jatkua pitkiäkin matkoja alueella. Samanlaiset vaihettumisvyöhykkeet ovat mahdollisia myös muualla lähiympäristössä.

Avainsanat: Migmatiitti, leukosomi, melanosomi, tekstuuri, Kilpisjärvi, metateksiitti, diateksiitti

Master's thesis

Subject: Bedrock geology
Author: Veeti Nurmi
Title: Migmatite textures from Kilpisjärvi region
Supervisors: Esa Heilimo, Jaana Halla
Number of pages: 54 pages + 2 appendices
Date: 27.2.2026

Migmatites are medium- to high-grade metamorphic rocks that contain a non-melted part and a melt-derived part. Paleosome is the part that has not been affected by melting and neosome is the opposite. Migmatite also contains a darker, melanosome part, and a lighter leucosome part. How these parts interact with each other form different textures, indicating different fractions of melt. By analyzing these textures, it is possible to interpret the origin and the protolith of migmatites, and how they link to the surrounding geology. The Kilpisjärvi area contains a largely unknown geological domain with unique structures and relationships between the different rock types. While the TTG migmatites do not extend into the younger Caledonian rocks, the older Archean basement includes these partially melted rocks. By researching the rocks in the area, it would be possible to refine the geological knowledge from Rommaeno complex and Kilpisjärvi.

The materials used in this study comprise of a set of images from Laassaniemi, Kilpisjärvi, rock samples and thin sections made from the rock samples. The samples show varying melting structures from nearly unmelted to completely melted with different strain environments also visible. The sample images present a boudinage structure and almost all the sample rock examples can be found within the structure. The size of the metatexite-diatexite transition zone is unclear but it is possibly laterally continuous and similar zones may occur nearby Laassaniemi.

Key words: Migmatite, leucosome, melanosome, texture, Kilpisjärvi, metatexite, diatexite

Contents

1 Introduction

Migmatites are a mixture of rocks containing at least two components that are petrographically different. The migmatites themselves can have varying textures depending on the melt-fraction and pressure present at formation. These textures are important in defining the origins of the migmatite melts and their compositions. Migmatite generally consists of a lighter part, leucosome, and a darker part called melanosome. The two can blend with each other in several ways forming characteristic structures. (Sawyer 2008)

The remote area of Kilpisjärvi and its geology have been a subject to few studies over the years. It is the only area in Finland to exhibit Caledonian orogenies and the Kilpisjärvi region also contains the highest peaks in Finland. These Caledonian formations are not a part of this study, but rather the ancient Archean rocks that are present to the south of the younger rocks as well as possibly below them. The Archean and Caledonian rocks have a 2 Ga discontinuity in between meaning, that there have been no major intermediate geological events. (Lehtovaara 1995)

The Laassaniemi area migmatites have not been studied before and their relation to the surrounding bedrock is unknown. In this study Laassaniemi area migmatite outcrops and eleven sample rocks are covered in detail. Eleven sample rocks were gathered from around the Laassaniemi area and thin sections have been made from all of them to further analyze the mineral composition and orientation of mineral grains. The goal of this study was to find out the relative age and origin of these migmatites and connect them to the surrounding geology as a whole.

2 General migmatite vocabulary

2.1 Components of migmatites

The term *migmatite* was originally introduced by the Finnish geologist Jakob Sederholm in 1907 to describe mixed rocks. The term comes from the Greek word *migma*, meaning "a mixture". This section follows the terminology, definitions, and classifications set out by Sawyer (2008), unless indicated otherwise. A migmatite is a medium- to high-grade metamorphic rock that contains two or more petrographically distinct components, with at least one component produced by partial melting. This melt-derived part is petrogenetically related to its protolith, either through *in situ* melting or segregation of melt from the solid fraction. The melt-derived component typically, though not always, has a paler color and is quartzofeldspathic or feldspathic in composition, whereas the darker parts are enriched in ferromagnesian minerals.

Figure 1 a-c shows a conceptual visualisation of migmatite vocabulary using a darker melanocratic protolith. **Paleosome** is the part of the rock that has not been affected by partial melting (Fig. 1a), and where pre-melting structures are visible and preserved. The microstructure has only slightly changed or has stayed intact compared to the rocks affected by anatexis. Paleosomes do not partially melt because of their composition, however it is not always clear what has melted and what has remained intact.

Melanosome (Fig.1a) is the darker part of the rock that is enriched in dark minerals such as orthopyroxene, hornblende, clinopyroxene, biotite and olivine. The melanosome is the solid, residual fraction left after the extraction of the melt fraction. Some microstructures indicating partial melting may be present. The melanosome represents the mineralogically reconfigured solid-state residual part of the rock from which the leucosome has been derived (Maxeiner et al. 2017). The best-known form in which the melanosome appears is along the *in situ* leucosome margin, but it is not the most common form it takes. It can also occur as patches, irregularly shaped bodies and continuous layers.

Neosome is the part of the migmatite that has been formed or reorganized during partial melting (Fig. 1b). Typically, the neosome has coarser grain-size compared to the rest of the migmatite and the pre-melting microstructures have degraded and eventually replaced by new microstructures as the degree of partial melting increases. The neosome is commonly subdivided into light-colored leucosome and darker melanosome.

In some cases, the leucosome and its protolith are separated by a narrow rim that is compositionally different from the surrounding rocks. This rim is called a **selvedge** and the reason for its formation is the chemical disequilibrium between it and the host rock (Fig. 1b). Three formation mechanisms have been proposed for selvedges: a reaction between host rock and an aqueous fluid exsolved when the melt that produced the leucosome or leucocratic dike crystallized, a reaction between the injected anatectic melt and the nearby wall rock and diffusive exchange of components between the anatectic melt and its host in response to activity gradients. Selvedges can be leucocratic, mesocratic or melanocratic, but the most common selvedge type is a biotite rich melanocratic rim called a mafic selvedge.

The lighter part in a migmatite is called a **leucosome** (Fig. 1c). It is mainly composed of feldspar and quartz, and it is derived from segregated partial melt. It can show microstructures indicating crystallization from a melt, or magma. Leucosomes can form *in situ*, in-source, or they can migrate away from their original position. An *in situ* leucosome crystallizes from an anatectic melt but remains at the melting site. It is in contact with its residuum, which can form a melanosome around the leucosome. An in-source leucosome has migrated away from the melting site but has not left the melting layer. As the in-source leucosome is not in contact with its original melanosome but remains in the same layer, the melanosome host will have a petrogenetic connection with the in-source leucosome. The melanosome might have formed from a slightly lower or higher degree of partial melting.

Resisters are the parts of the migmatite that remain unchanged even into the highest-grade migmatite parts (Fig. 1c). Common resisters are calc-silicate rocks, quartzite and metamafic rocks. Resisters have higher melting temperatures compared to surrounding rock because of their unusual composition. Because of their extreme bulk compositions, the resister rocks have not melted under the same P-T conditions that have melted the surrounding rock (Maxeiner et al. 2017).

If the leucosome leaves the melting layer it is considered a leucocratic vein or dike, or a granite dike or sill. The leucocratic veins commonly present sharp contacts with the host and there is no direct relationship between the vein or dike and the host rock surrounding it. The age of the crystallization of the vein or dike should however correlate with the metamorphic age of the host. Granite dikes have sharp contacts with their host rocks as well, and they may also have fine-grained border zones called chilled margins. There is no relationship between the granite dike and the surrounding rock. The dike may have formed from the crystallization of intermediate, felsic, or even mafic magma.

Leucosome and melanosome parts are more easily distinguishable from each other if the protolith is a darker rock such as a metagreywacke, metadiorite or a metamafic rock, but if the rock is more leucocratic the dilution of the mafic minerals by feldspar and quartz can produce only subtle changes in color making separation by color harder. In a situation where the melt fraction and the solid fraction do not separate and clear leucosome and melanosome do not form, the term neosome can be used alone.

The term **mesosome** has been used for rocks that are not melanocratic or leucocratic, but due to its ambiguity it is not recommended to be used. More specific terms are used instead.

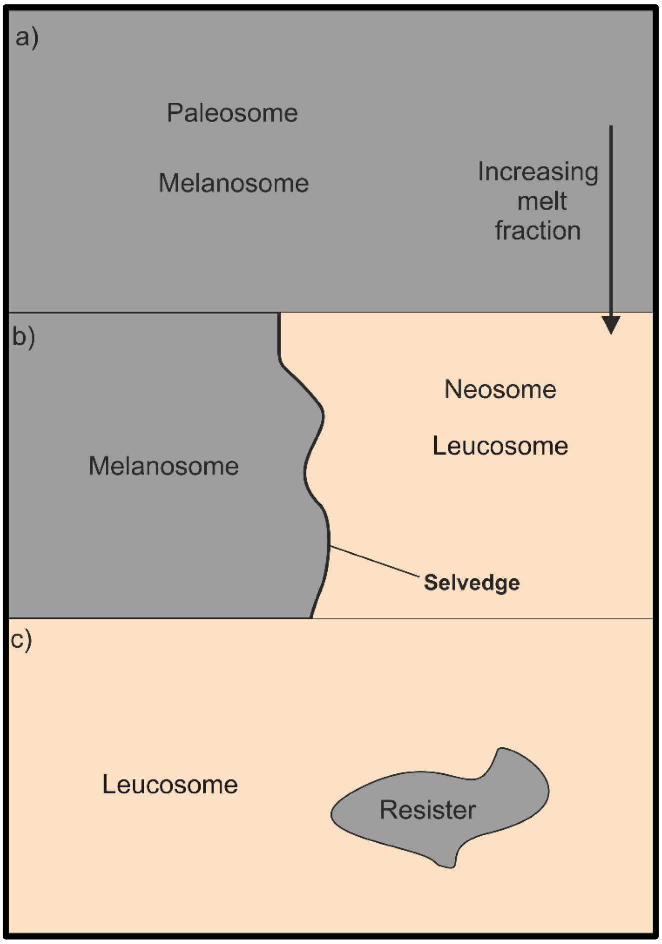

Fig. 1: Migmatite vocabulary illustrated using a darker melanocratic protolith. a) The rock has not melted and is intact. b) Partially molten rock showing distinct darker melanosome and lighter leucosome; the melted portion is referred to as a neosome. A selvedge occurs between the melanosome and leucosome and has a composition different from both. c) rock that has mostly melted, leaving only the more resistant components.

2.2 Migmatite formation by partial melting

Migmatite formation by partial melting generally happens under differential stress (Sawyer 2008). Crustal rocks deform heterogeneously, ultimately creating stress differences which form pressure gradients. After deformation has made the matrix permeable enough, the melts start moving upwards or downwards, collecting in nearby low-pressure areas. If the differential stress at the crustal melting site exceeds the amount needed for permeability, the additional fraction of melt would move to low-pressure sites nearby. This melt segregation process is a relatively non-destructive process, as even some of the granulite-facies migmatites can still include preserved sedimentary structures. In special cases, partial melting leading to migmatite formation can happen under lithostatic stress conditions. These conditions do not have enough force to drive the melt out of the solid framework, which then leaves the melt and the solid together. The neosome remains isotropic, and leucosome and melanosome will not separate. After enough melting has occurred, the contacts between solid grains vanish, and a very weak rheology is created. If convection or gravity separation of heavy minerals occurs, then separation and orientation of minerals are possible.

2.3 Principles of migmatite classification

The division of migmatites specifies distinct structures in metatexites and diatexites according to the structural features formed during partial melting. Figure 2 shows how the combination of syn-anatectic strain and melt fraction forms different types of migmatites (Sawyer 2008). The strain used in the division is qualitative and separates less deformed rocks from more deformed ones. Usually, higher strain migmatites show simpler morphologies, since the whole migmatite has been weakened and strongly transposed. Migmatite characterization based merely on strain would not provide a precise enough division to distinguish metatexites and diatexites from each other. The differences in morphology in diatexites are mainly based on the melt fraction of the migmatite, as the strain amount needed for flow structures and foliation is rather low, and higher strain only defines preferred orientations.

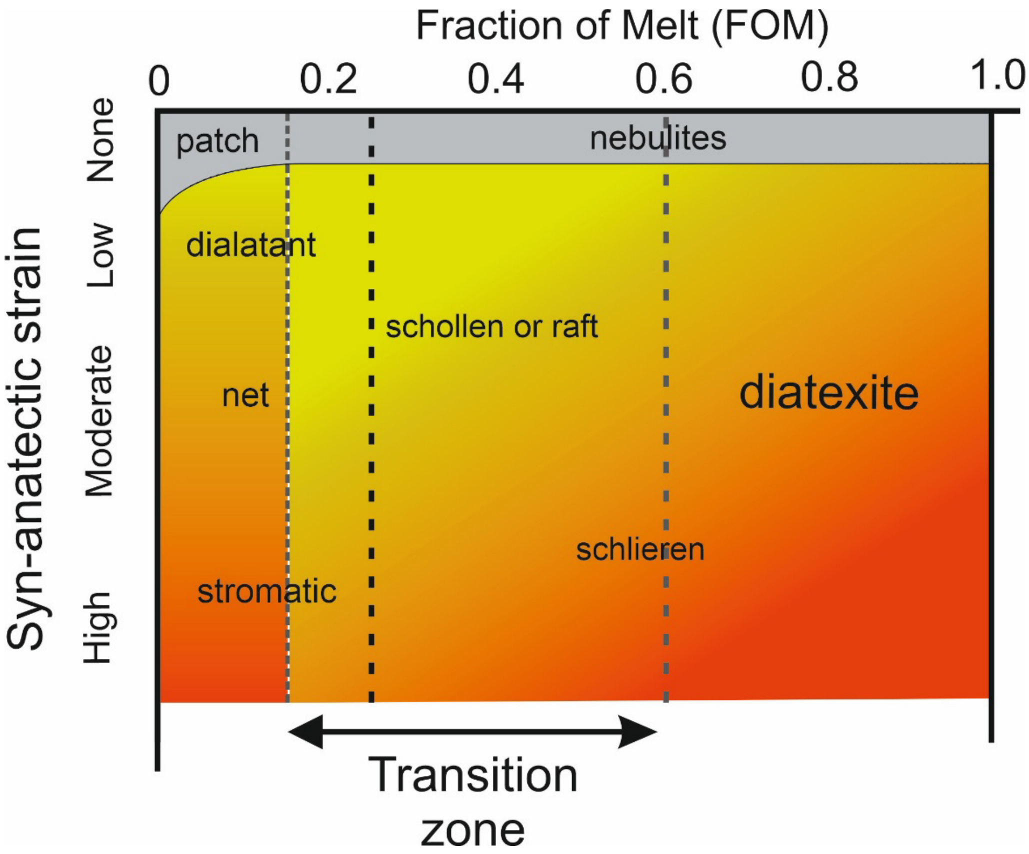

Fig. 2: A classification scheme for migmatites. The second-order division includes syn-anatectic strain on the y-axis and the fraction of melt on the x-axis. The black dotted line represents the transition of metatexite into diatexite in the Uniform Rigid Spheres (URS) model and the two grey lines represent the nonuniform shape and size model (NUP) transition zone. Modified after Sawyer (2008).

2.4 Migmatite morphologies, structures and textures

2.4.1 The effect of melt fraction

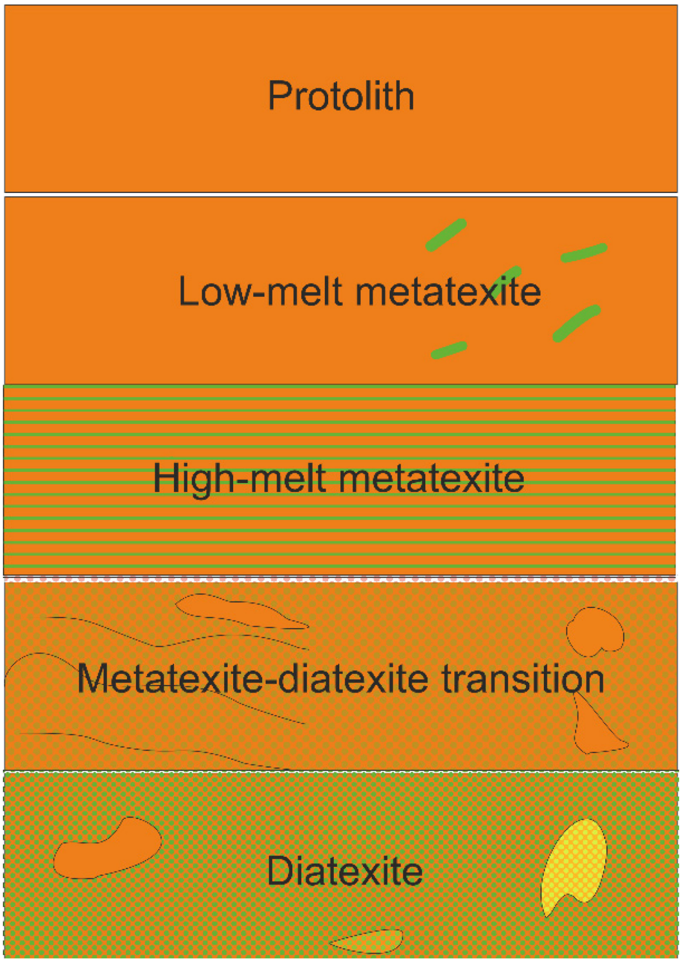

Fig. 3: Migmatite morphologies and structures at different melt-fractions starting from 0% melt where only the original protolith is present. Low-melt metatexite exhibits patch migmatites while remaining mostly intact. High-melt metatexite includes dilation structures and layered or folded metatexites. Metatexite-diatexite transition features raft- and schlieren structures with increasing melt migration and strain. Lastly, diatexite is composed of melt redistribution structures, flow-banding, and vestiges. Zhang et al. (2019) modified after Halla et al. (2024).

2.4.2 Metatexite migmatites

In the lower-grade parts of anatectic terranes, paleosome is dominant and the structures predating partial melting are preserved. The neosome is characterized by randomly oriented leucosome bodies, bordered by melanosome (Sawyer 2008). The migmatites formed in low degrees of partial melting are called metatexites. They contain 26 to 60% neosome and they are structurally cohesive (Maxeiner et al. 2017). As the anatectic grade rises, the neosome parts become dominant and leucosome is highly abundant compared to residual material. Paleosome is rare and sometimes even absent, and original textures before anatexis have been replaced by syn-anatectic structures.

The low melt-fraction, low-strain migmatites are generally hard to notice, as the morphologies formed are subtle (Sawyer 2008). The first signs of partial melting can be fine grained quartzofeldspathic films, which represent crystallized melt. Pink coloration at the edge of some muscovite grains has also been found by Holness and Watt (2002). Although the metatexite migmatites may have lost their original textures completely, they should not be referred to as diatexites, because they are mainly tectonically formed (Sawyer 2008).

Patch migmatites are formed in an environment, in which scattered melting occurred so that a patchy texture has formed. The neosome patches are round or oval and surrounded by dominating paleosome. Oriented bodies can form if melting is limited to thin layers. Neosome patches can mend together at higher degrees of partial melting. These migmatites can be called nebulites and, as can be seen in Figure 2, they have a melt fraction of 0.26 to 1.00. Patch migmatites are normally mesocratic, meaning that the leucocratic and melanocratic parts have not separated. However, if the melt and residuum do separate, melanocratic and leucocratic structures start forming. Patch migmatites are found the most in low syn-anatectic strain environments. Because patch migmatite contains nascent melting, the rocks are also stronger and more competent. This is why patch migmatites can withstand more syn-anatectic strain than nebulitic migmatites, visualized in Figure 2.

In **dilation-structured migmatites**, the leucosome is situated in, as the name suggests, places such as pressure shadows or fractures. The sites are not large, and are restricted to specific layers, which indicates the competency differences between the layers in the migmatite. The more competent layers are usually quite barren, but it is possible that they represent newer residual layers, which are rich in strong minerals such as garnet.

Net-structured migmatites are considered as a good partial melting indicator. They consist of two or more sets of leucosome bands that form a net-like pattern which outlines the diamond-shaped or polygonal blocks of darker rock. The net-structure often develops after one or several sets of extensional shear bands in which the leucosome is located. It can be recognized by the curvature of the foliation from the host rock to the leucosome. The anatectic melt concentrates in the shear bands in the nearby area as the rock undergoes layer-parallel extension. The melt might migrate into the shear bands or away from them depending on whether the shear band is extending or shortening. These shear bands are typically parallel to the prevailing layering or foliation. The distinct melanosome around the leucosome bands starts to disappear with increasing partial melting. The diamond-shaped paleosome blocks slowly transform into neosome as the partial melting increases. If the melt fraction further increases, these net-structured migmatites may transition into raft or schollen diatexite migmatites.

The highest grade syn-anatectic strain forms **stromatic or layer-structured** migmatites (Sawyer 2008). These layers have a similar orientation to the major plane of anisotropy and the leucosome bands generally have parallel melanosome bands surrounding them. An *in situ* origin has been proposed for these types of migmatites, because the residual composition of the melanocratic bands is not appropriate for an injection origin. Also, the melanocratic part of the layered migmatites is the residuum left after the partial melt has been extracted, and the composition of the melanocratic area is similar to the adjacent leucosome, which further supports the *in situ* origin (Sawyer 2008).

2.4.3 Metatexite-diatexite transition

The near-complete fusion migmatites, where neosome is clearly the dominating part, are called **diatexites** (Mehnert 1968). According to Maxeiner et al. (2017) they contain over 60% neosome and have lost most of their structural cohesion. Sawyer (2008) notes that the metatexite-diatexite transition is model-depended. In a model, where solid crystals are treated as uniform, rigid spheres (URS), the transition happens at melt fraction of 0.26, but for a model that handles solid particles as nonuniform in size and shape (NUP) the transition zone extends from 0.16 –0.60 melt fraction (Sawyer 2008).

For diatexite migmatite formation, two aspects need to be considered: How the pre-anatectic structures have been replaced by syn-anatectic structures, and how the large, high melt-fraction domains form (Sawyer 2008). Once the rock has melted enough, the intergranular contacts disappear in the matrix and the rock becomes a suspension of crystals in the melt, i.e., magma. Once the magma starts flowing, in response to the shear stresses created by tectonic forces, the pre-partial-melting structures are replaced by structures formed by magma flow, and diatexite migmatite is produced. A domain containing a high melt fraction must form so that new melt is produced faster than it can migrate away from its source. This rapid melting might be caused by the influx of aqueous fluid.

The microstructures in diatexites show that some have flowed as suspensions of crystals in a melt, and some have generated their microstructures after the flow in the crystallization phase (Sawyer 2008). There are several different ways in which diatexites can form in a closed or open system.
In a closed system, where the degree of melting and the melted fraction are clearly under the solid-to-liquid transition (SLT), there are two possible ways to form diatexites. Firstly, mechanisms such as grain-boundary sliding, melt-enhanced diffusion, and dissolution may lead to bulk flow (a flow of a solid containing a small amount of melt). Secondly, increasing temperature may cause the degree of melting to rise above the SLT, leading to the formation of magma flow. Thirdly, if the system is closed on a larger scale, but locally open, diatexite can form from the movement of anatectic melt within the migmatite, because this increases the melt fraction regionally over the SLT zone, causing magma flow.

In a case where the system is completely open there are two possibilities for diatexite formation. One possibility is that granitic magma flows from an outside source and intrudes into the migmatite, which then augments the local anatectic fraction so that the melt fraction rises above the SLT and makes magma flow possible. The other possible formation environment is when aqueous fluid is combined with already high temperature rocks, which raises the melt fraction rapidly over the SLT.

Nebulitic migmatites

Above 0.26 melt fraction, the foliation in migmatites starts to disappear, and unsegregated neosome starts forming (Sawyer 2008). In some cases, it is possible that the nebulitic migmatites begin forming before reaching the above-mentioned melt fraction if the melting happens evenly in the whole protolith. Nebulitic migmatites are often fragile, as they only appear in places where the syn-anatectic strain is very low.

The textures appearing in these migmatites are often caused by magma flow because of the absence of strain.

Rafts and schlieren diatexites

As the strain increases, raft-like paleosome, resisters, or melanosome structures start forming (Sawyer 2008). This type of diatexite is common in the transition from metatexites or from lower melt fraction diatexites. The paleosome component is most abundant near the transition zone. The rafts are originally large and usually show little rotation, but as the conditions move towards the diatexite zone, the rafts start decreasing in size, and they are more rounded and dispersed in the leucocratic neosome. The leucocratic areas have flow foliation that is aligned with platy minerals such as feldspars. These migmatites are also called raft migmatites (Fig. 4).

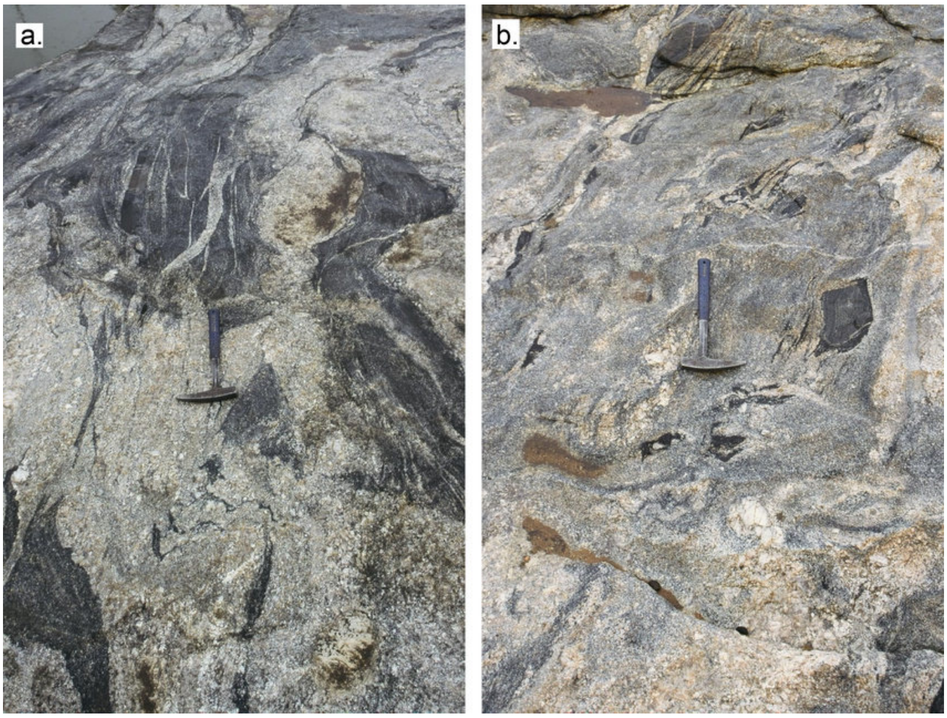

Fig. 4: Raft and schlieren textures from the Pilbara Craton containing large blocks of paleosome appearing to have been broken apart by the flowing melt (Pawley et al. 2013).

Schlieric migmatites (Fig. 5) start forming as raft migmatites increase in melt fraction (Sawyer 2008). The name schlieren comes from stretched minerals, usually biotite but can also be sillimanite, plagioclase, orthopyroxene or amphibole. Raft paleosome may be present, but it is far less common than in raft migmatites. Strain has no effect on raft-schlieren transition (Sawyer 2008).

Fig. 5: Biotite schlieren textures from Coz Porz beach, Brittany, France. They can be seen in the image as slivers of melanosome that have flowed within the larger leucosome (Mindat 2018).

2.4.4 Diatexite migmatites

Diatexite migmatites are the highest melt-fraction migmatites (Sawyer 2008). They are dominated by neosome, and paleosome is rare or absent. Foliation oriented parallel to platy or tabular minerals, formed from magma flow, is pervasive, and structures from before the melting are only found in tiny paleosome rafts. Diatexite migmatites form from raft and schlieren migmatites, through melt-fraction increase, and from nebulites through syn-anatectic strain increase. Diatexite migmatites contain, almost without exception, leucocratic veins or patches comprised of quartz, K-feldspar and plagioclase. They pre-date the flow structures in their host rocks. Because of the high melt-fraction in diatexite migmatites, the crystals in them align under differential stress and form a foliated structure. Increasing strain generates refined alignment of minerals, rafts, and schlieren. Residual melt may segregate if deformation happens during crystallization, which leads to well-developed planes of foliation or compositional banding (Sawyer 2008).

2.4.5 Other migmatite morphologies

Two migmatite structures that fall outside of the metatexite-diatexite division are vein and fold structures (Sawyer 2008). The vein structures form depending on the type of fracturing, brittle or ductile, and the timing of the veining processes relative to the rest of the tectonic history, while the folding structures form differently in metatexites compared to diatexites.

Fold-structured migmatites

Migmatites with fold structures are created at low melt fractions and in the early stages of anatexis (Sawyer 2008). The morphologies in fold-structured migmatites are controlled by competence differences between the layers in the paleosome. More competent layers can form buckle folds next to the more incompetent layers. As the folding advances, a part of the melt migrates into the dilatant sites created, for example leucosome accumulating in fold hinges and parallel to and between the folded layering. It has been noted that fold hinges contain more leucosome than fold limbs, indicating that limbs could be net loss regions of melt, while the hinges are net gain regions. The folds transition from cylindrical and planar to noncylindrical, nonplanar and disharmonic folds after passing the melt escape threshold (0.26 –0.40 melt fraction). With fold-structured migmatites, it is important to study microstructures, as they reveal if the fold structures formed during a high melt-fraction phase or later during crystallization and lower melt-fractions, as the structures may look quite different. It is also possible that the folding has occurred in a completely solid state, which makes the rocks folded migmatites and not fold-structured migmatites (Sawyer 2008).

Vein-structured migmatites

Vein-structured migmatites have one or several generations of discordant leucocratic veins, which have formed on top of older metatexite or diatexite morphologies. The youngest vein structures are typically younger than the peak anatexis and are undeformed. Some common microstructures in vein-structured migmatites show indications of melt injections into partially molten wall rocks and of vein wall erosion. Narrow mafic selvedges are usually found on the borders of the veins, which may have formed by a reaction between the injected melt and the wall rock or with a fluid derived from the melt. Although the youngest veins have formed after the peak anatexis, they are still derived from the same anatectic event as the rest of the migmatite. If the veins are from a younger event, the migmatite is called a veined migmatite instead of a vein-structured migmatite.

3 Regional geology

Kilpisjärvi region is situated on the border of North-West Finland, North-East Sweden and Northern Norway (Fig. 6). The region also incorporates the highest peaks in Finland and nearly all of the peaks above one kilometer in the whole country. It belongs to the Norrbotten geological province, which mostly formed during the Svecokarelian orogeny (Bergman 2018). The Archean basement rock represents a far older development phase. The Caledonian mountains, which are mostly located in Sweden and Norway, extend to Kilpisjärvi, making it the only area in Finland to exhibit them. The Caledonian cover in the North-West and the Archean basement rock in the South-East are separated by an unconformity zone. It is also a part of the Rommaeno Trondhjemite-tonalite-granodiorite-amphibolite terrain (Halla 2020). This complex is composed of migmatitic banded and folded TTGs and amphibolite rafts and enclaves.

The Rommaeno Complex is mostly unexplored as the remote location makes it a difficult area to map. The tectonic processes responsible for the transformation of Archean basaltic crust into TTG suites remain debated (Halla 2020).

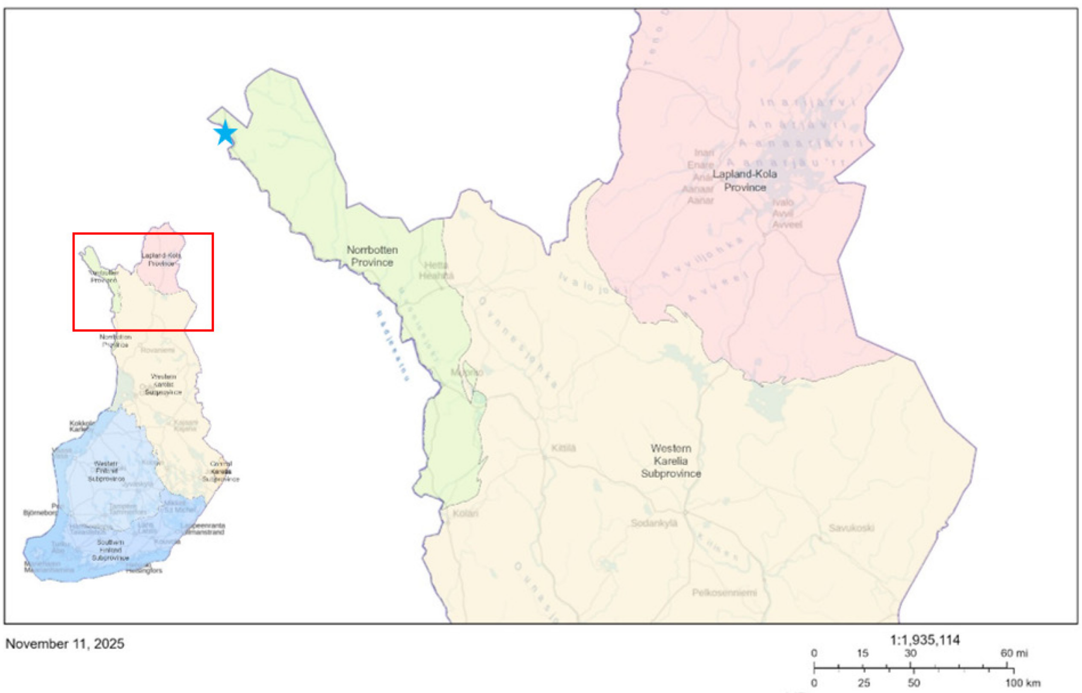

Fig. 6: Location of Norrbotten province and Kilpisjärvi on a map. Norrbotten province is visualized with light green color at North-West Finland, while Kilpisjärvi is shown as a light blue star.

3.1 Kilpisjärvi stratigraphy

The Kilpisjärvi region is separated into two distinctively different areas, bordered by a 2 Ga discontinuity zone in between called the Dividal Group (Lehtovaara 1995). What makes Kilpisjärvi unique is that it is the only place in Finland exhibiting the Caledonian mountain belt. (Lehtovaara 1995). Beneath the Caledonian allochthon is Archean bedrock, which has not been affected by the Caledonian Orogeny (Matisto 1969). The Caledonian formations in North-West Finland have characteristic subhorizontal to gently dipping allochtonous thrust sheets.

The oldest parts of the Kilpisjärvi area are the Archean gneisses, dated to around 2.7 to 2.8 Ga. It contains granodiorites with varying gneissic features, which can also partly be tonalitic and granitic (Lehtovaara 1995). Primary features are missing from these ancient rocks, but some micaceous gneiss inclusions are visible. The Archean basement has been crosscut by possibly Proterozoic uralite diabase veins, which are SE-NW oriented (Lehtovaara 1995). The ages of these veins are merely relative calculations based on crosscuts and the location of them. The absolute ages are unknown.

The Caledonian area can be split into subgroups stratigraphically. The Dividal Group forms the base of the area, comprising of sedimentary rocks that start with a basement conglomerate, formed at around the end of Precambrian. The top of the formation is Cambrian in age, and while Ordovician structures are found on the Norwegian side, none have been found in Kilpisjärvi (Lehtovaara 1995). As the study area is completely on the Archean side of the region (Fig. 4), further details of the Caledonian rocks will not be discussed in this study.

3.1.1 The Archean rock types of Kilpisjärvi

The name of the Archean basement gneiss complex is a generalization as it is similarly aged compared to the bedrock of Eastern Finland (Lehtovaara 1995). Most of the basement gneiss complex is composed of three main granitoid rock types: Granodiorite, monzogranite and granite, which appears typically pegmatitic. The origin of these granitoid rocks is not known because of the absent primary textures and the migmatitic nature of them (Lehtovaara 1995). The main minerals in the basement gneiss granitoid are plagioclase, quartz, K-feldspar and biotite. Especially the varying biotite content in rocks is a major factor in defining rock types. The absence of garnet is a defining characteristic in the whole basement gneiss. Muscovite, chlorite and hornblende can appear occasionally. Epidote, titanite and apatite are present as alteration products.

Mica gneiss is present only rarely and generally as inclusions in the granitoids and the mica content is highly variable in the area (Lehtovaara 1995). It is fine grained at 1 to 2 mm, and combined with high biotite levels, it is a criterion in defining rock types. The biotite content can rise to 30% and can create strong schistosity.

Medium to coarse grained gneiss with a very high content of hornblende has been found near Saivaara. It has most likely been metamorphosed thoroughly and differentiated, leading to partial melting of the basement gneiss complex. Some equigranular amphibolite is featured in the basement gneiss area. Originally, it may have appeared as layers in between the gneiss, but today it exists as inclusions adapting the orientation from schistosity. Occasionally, decreasing hornblende and increasing biotite portions alter it to mica gneiss and alternatively some epidotization and chloritization are also present. Salmivaara metavolcanic unit is the biggest amphibolite belt in Kilpisjärvi area. It begins on the eastern side of Saanatunturi and continues north-west toward the Caledonian allochthon. The phase is around 5 km long and 1km wide.

3.1.2 The study area

The Laassaniemi area (Fig. 7) is mainly located on granodioritic grounds with minor mica gneiss and basic metavolcanite. Most of the Kilpisjärvi area is granodioritic, but K-feldspar percentages vary heavily so the rock composition can fluctuate. Rock contacts are rarely defined since the basement gneiss is chiefly a mixture of different gneiss variations, with migmatitic and even nebulitic textures. A typical granodiorite is directional, and biotitic mineral lineation is parallel to it. It is medium grained from 3 to 5 mm, equigranular and mostly plutonic (Lehtovaara 1995). The textural heterogeneity of the Laassaniemi area makes it a suitable migmatitic setting for examining variations in the degree of partial melting.

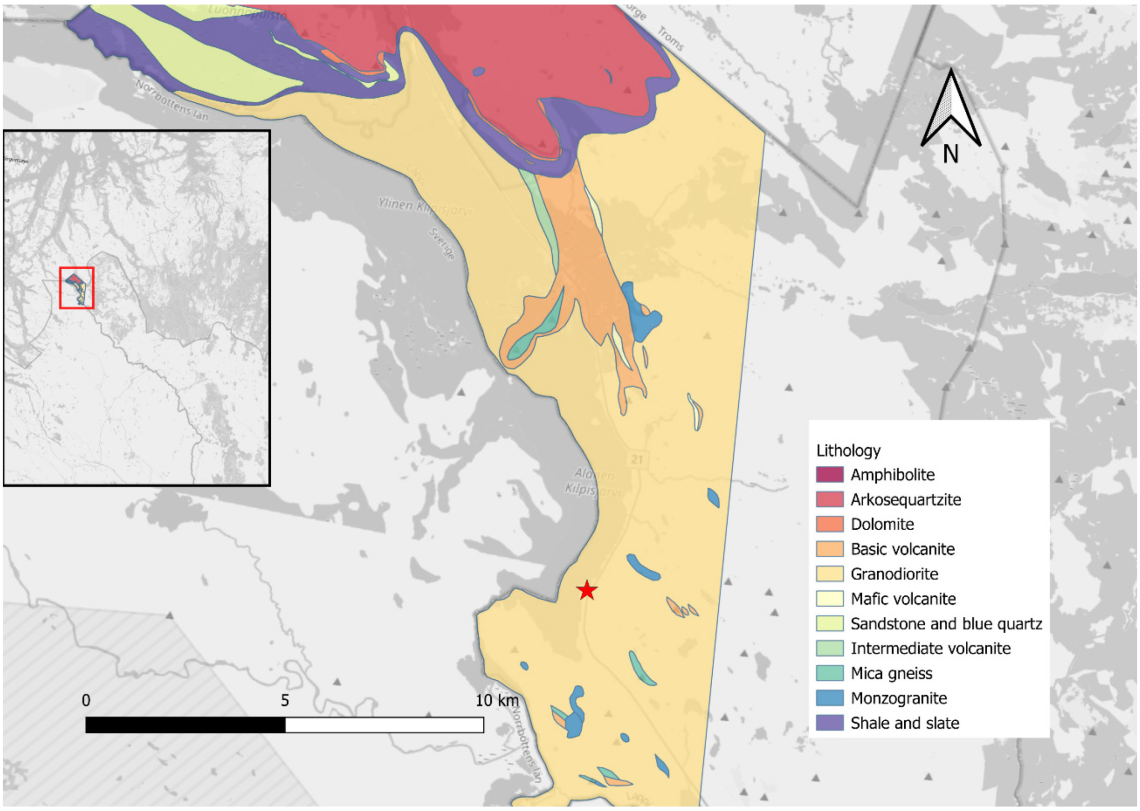

Fig 7: Location of Kilpisjärvi on the map with local rock types. The red star represents Laassaniemi, the study area. The area is mostly surrounded by granodiorite with minor mica gneiss and volcanite nearby. Laassaniemi coordinates: 68°56.5082'N, 20°54.7202'E, Elevation 485m (Lehtovaara 1995).

4 Materials and methods

The on-site images have been taken from a roadcut next to the Käsivarrentie road and a loose boulder on the western side of the road. The rock sample images were taken with a high resolution digital camera and using Lightroom image editing software for contrast and clarity. For thin section imaging, a microscope with a camera was used and the microscope lens magnification was between 2.5x and 6.3x for all images.

Texture analyses were made from images, rock samples and thin sections from the study area (see Fig. 7 for sample locations) with particular emphasis on the spatial relationships between leucosome, melanosome and neosome. The thin sections used were cut from the sample rocks (Fig. 8) using a rock saw and then analyzed with an optical microscope. In total, 11 rock samples were collected for this study, from which the thin sections were made. These samples have been taken in three groups and sorted according to the location of the sample site.

Fig. 8: The sawed rock pieces used to make thin sections.

The sample images have been separated according to the image size. Beginning from the largest, sitewide images and ending in microscopic thin section photos. The largest scale images will be covered separately as they are not possible to link directly to the sample rocks used in this study because the sample rocks have been taken as blasting debris.

5 Results

The observations presented below are therefore descriptive and textural in nature. This chapter is split into subchapters, segregating the structural images and the sample rocks from each other. As stated in Chapter 4, the structural images taken at Laassaniemi are not comparable to the sample rocks used in this study, as the rocks are explosion debris formed as a result of excavation.

5.1 Outcrop image analysis

The images taken from the roadcut at Laassaniemi show varying textures and structures. The complete roadcut image can be found in Appendix A with complete textures pictured in Appendix B. This chapter analyses the structure of this roadcut in pieces starting from the southern end of the roadcut (right side of the image) and continuing left. The name Laassaniemi gneiss has also been used by Karinen et al. (2015) for the same migmatites. The age of the tonalitic orthogneiss has been estimated to be 3215±3 Ma (Karinen et al. 2015).

Figure 9 displays two melanocratic blocks on the right side of the image, which have been cut by a leucocratic, rather schlieric horizontal structure. The melanocratic blocks appear texturally older than the surrounding leucocratic material and they can potentially represent larger raft structures. The base of the structure is made up of amphibolite, and the leucocratic melt has migrated from the top layer and blended to the bottom layer. The amphibolite layer is quite heterogeneous with leucocratic material, and the horizontal schlieric structures dominate the middle part of the layer with some leucocratic raft structures on the right side of the measuring stick. On the left side of the same measuring stick, a heavily folded leucocratic vein advances sub-horizontally, showing cross-cutting relationships with the surrounding schlieric structures. Between the lower neocratic layer and the upper leucocratic layer is a darker thin layer, which shows less directional structures than the bottom layer. It has also been intruded by the leucosome melt from the top layer causing vertical “spikes” of leucocratic material on the left side of the measuring stick.

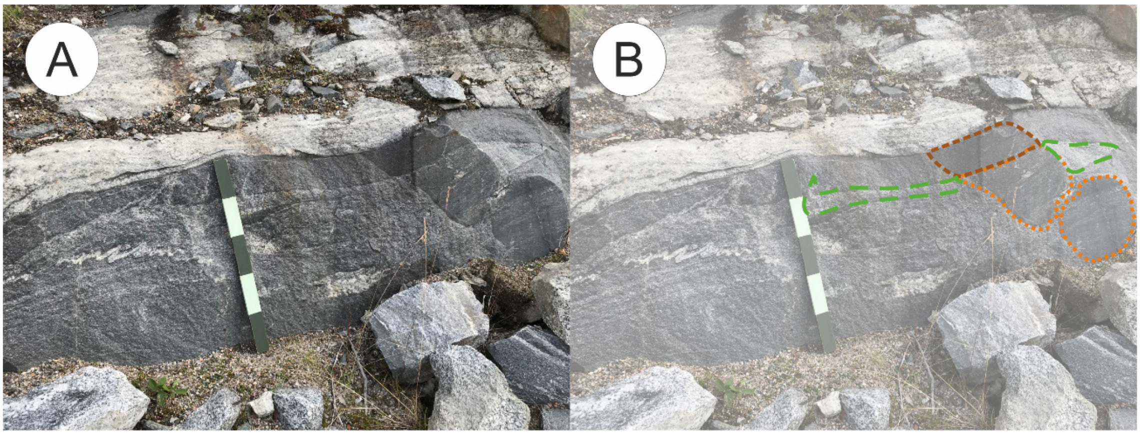

Fig. 9: The rightmost side of the roadcut at Laassaniemi (A) and the structures colored accordingly in (B). Some flow banding, raft structures, and schlieren can be seen in the images with apparent ages of melanosome predating the leucosome.

Figure 10 is taken to the left of Figures 9 and 10B visualizes the textures. On the left side of the image, a boudinage structure gap is displayed and the prevailing structures seem to follow this structure. In Figure 10B the green color represents the leucocratic parts, while the orange color represents the melanocratic. In the middle of the image, to the left of the measuring stick, is a mixture of the upper leucocratic layer and the lower melanocratic layer. The leucocratic material occurs within the melanocratic layer and extends laterally along it. In the lower part of the melanocratic layer, on the bottom right of the Figure, a raft of leucosome has formed. In the lower, Figure 11, the boudin structure is visualized quite clearly, with veins bending according to the structure. To the left of the measuring stick ptygmatic leucosome folding (Weinberg 2016) can be seen. The intruding leucosome vein has entered the melanocratic amphibolite from the boudinage formation pressure shadow

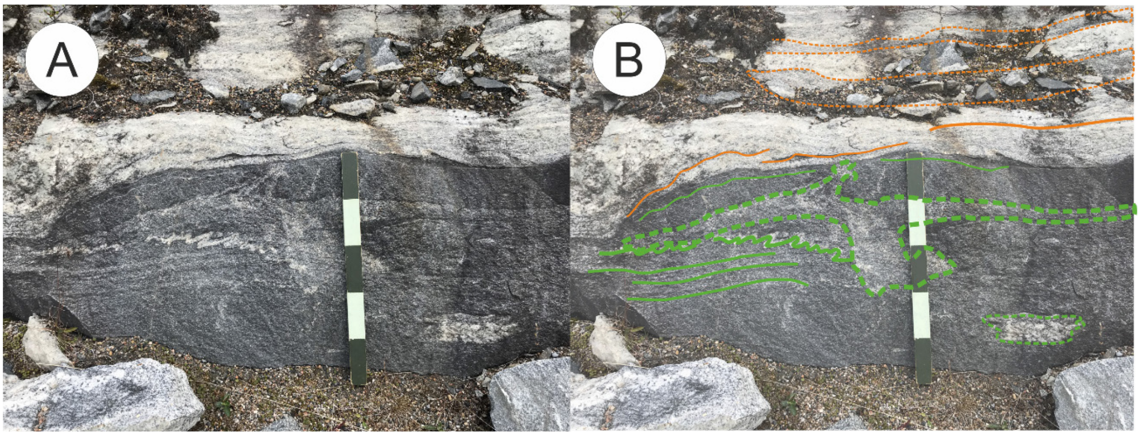

Fig. 10: The southern side of the boudinage structure in Laassaniemi exhibiting schlieric leucosome and ptygmatic folding.

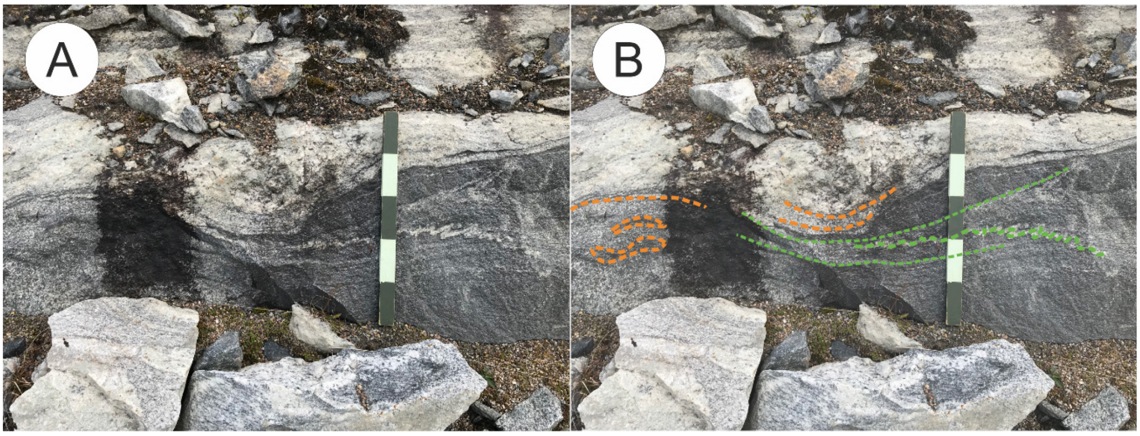

Fig. 11: The middle section of the Laassaniemi roadcut featuring boudinage textures and amphibolite-nebulite transition. The green color represents leucocratic textures while the orange color represents melanocratic textures.

In figure 12, the prevailing base rock has transitioned into nebulite in the roadcut. Some elongated raft structures of melanosome can be perceived on top, while other melanocratic, almost schlieric structures are also visible. A pure leucosome raft can also be seen at the bottom left of the image (drawn in green in Fig. 12b).

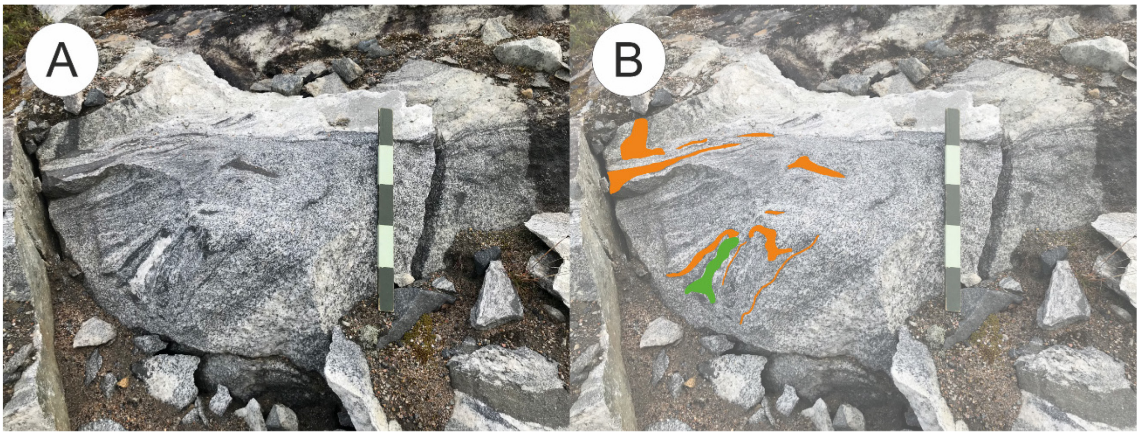

Fig. 12: The left corner of the roadcut at Laassaniemi. The background structure in this image is nebulitic, and the nebulite contains rafts of melanosome behaving like relict rafts.

5.1.1 Other findings

In this chapter, the rest of the findings from Laassaniemi area are listed as photographs and other observations. Figures 13 through 15 represent the general textures of the rest of the area excluding the previously mentioned roadcut in Appendix A. The location of these images is not certain, but they have been taken in the vicinity of the Laassaniemi roadcut, so it is highly probable that they are connected to the nearby migmatites in some way.

Figure 13 shows a complex melt structure with intact unmelted fragments of melanosome. Excluding the intact fragment on the left side of the image, the rest of the outcrop appears to be heterogeneously mixed depending on the base rock composition. In more melanocratic areas the leucosome has seemingly mixed quite homogeneously among the melanosome, forming a nebulitic structure, while the leucocratic veins span the whole outcrop horizontally flowing around the nebulitic piece in the middle of the outcrop. The melanosome appears to predate the other structures. The nebulite has formed after that with the leucocratic veins forming last, penetrating the former structures and flowing around the melanosome fragment.

Fig. 13: A boulder in Laassaniemi exhibiting migmatite textures. The image is oriented facing south with the rock face striking east-west. The leucocratic veins range from a few millimeters to over 10 cm in thickness.

Figure 14 displays a less complex banded structure compared to the irregular and heterogenous Figure 13. The banding in this outcrop consists of a schlieric layer at the bottom with slightly greater amounts of leucosome. On top of this is a mostly melanocratic layer with minor amounts of leucosome. This layer is difficult to interpret as the white texture can also be weathering. The edges of this layer appear to be more melanocratic than the middle suggesting that the layer has been melted from the middle outwards. These edges break apart from the layer on the left of the outcrop. On top of this layer is a heavily heterogeneous layer of schlieric melanosome structures in a melanosome layer. Some rafts also appear on the left side of this layer.

Fig. 14: An outcrop in Laassaniemi area with migmatitic textures.

In Fig. 15 a fault is visible that has experienced slight vertical movement along the fault plane. This fault formed after the leucosome patch in the bottom half of the image, but the melanosome appears to have invaded the crack formed by the fault. The rest of the image is quite heterogeneous, and the textures appear to be directional and diatexitic. The composition changes from more leucocratic at the top of the image to more melanocratic at the bottom. No apparent layering is seen and the composition changes gradually. Some weathering is seen to the right of the measuring stick and the fault.

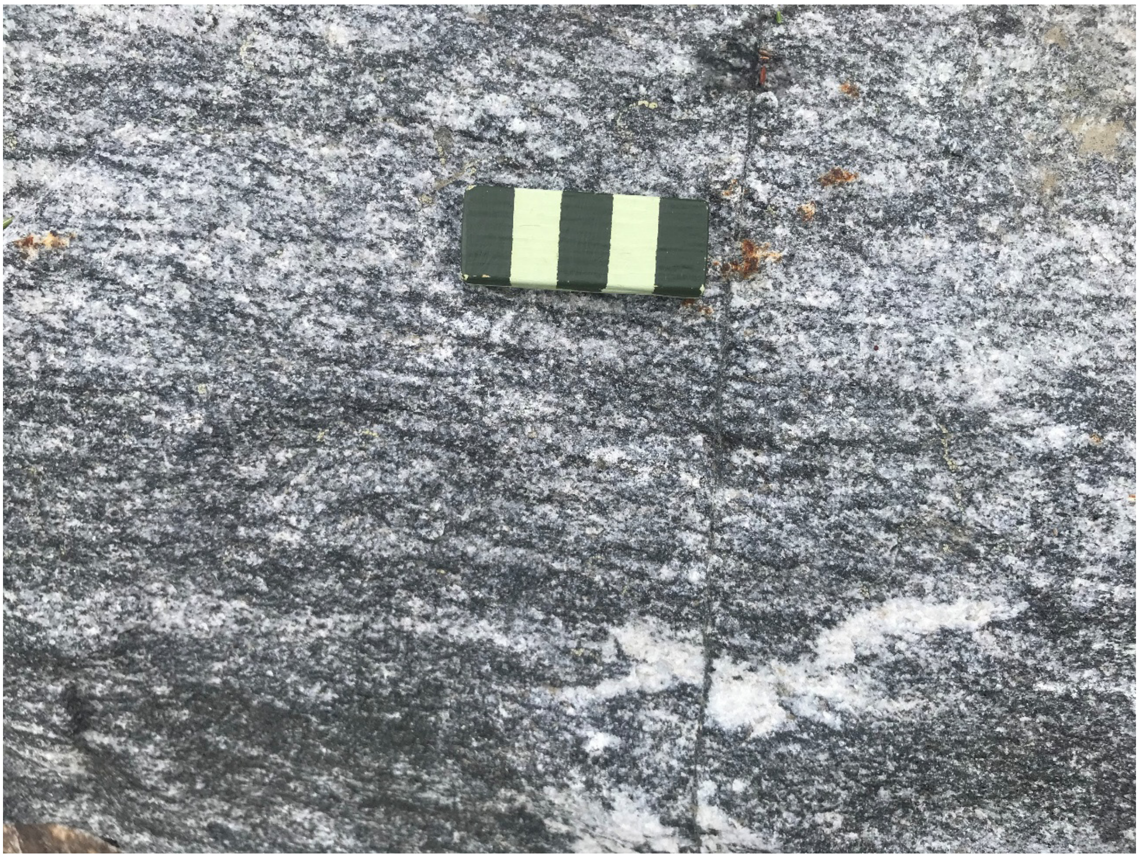

Fig. 15: A boulder from Laassaniemi area with migmatitic textures.

5.2 Macroscopic description of samples

The rock samples are divided into three groups according to their structural position within the Laassaniemi outcrop. Each of these groups represent a specific melting phase at Laassaniemi and eleven hand samples were collected in total. The rock samples contain diverse textures, and no clear dominance can be perceived between melanosome or leucosome. Usually, leucosome veins are injected into the melanosome, suggesting a greater relative age of the melanosome compared to the leucosome.

5.2.1 Laassaniemi 1

Sample 1A (Fig. 16) presents a melanocratic base structure with irregular leucocratic patches or domains. The sample is dominated by melanocratic material with only minor isolated leucocratic patches, suggesting low strain. The grain size of the melanosome is small, and the raft structures range from around 0.25 cm to almost 2 cm in diameter.

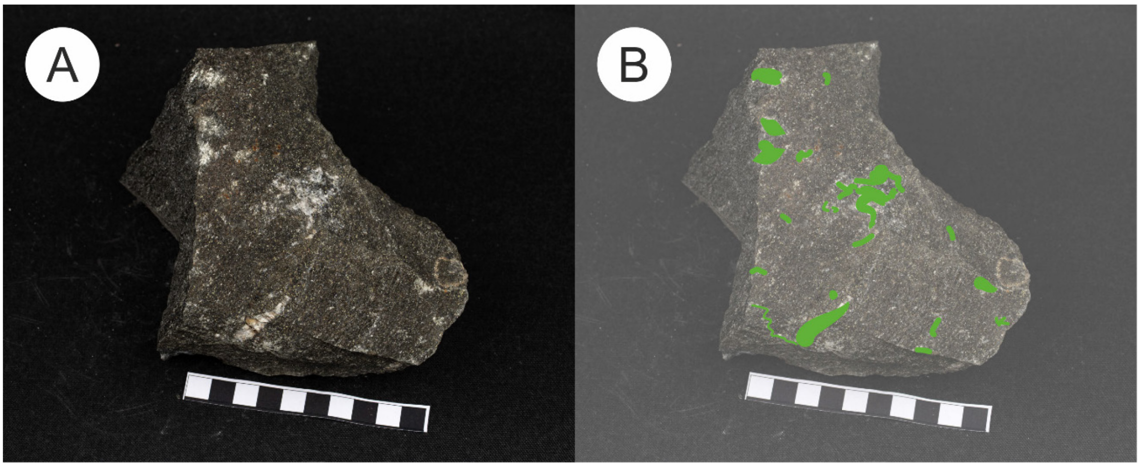

Fig. 16: Sample 1A (A) and its textures visualized in colors (B). This sample represents low leucosome-fraction migmatite with most of the sample being melanosome.

Figure 17 shows sample 1B and exhibits its features in colors on the right. This sample appears to be a mixture of several attributes, with leucosome, melanosome and neosome present. The different parts have only slightly merged and have generally stayed separated. This sample represents the high leucosome-fraction rocks of the area, while still having, intact pieces of the original rock. The average grain size of the sample melanosome is around 0.5 cm with some larger grains reaching 2 cm in diameter.

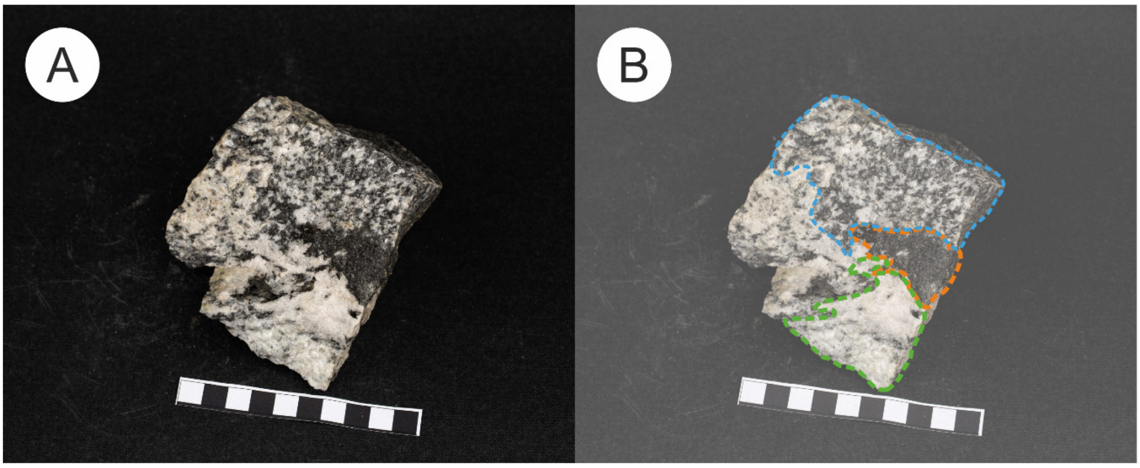

Fig. 17: Sample Laassaniemi 1B (A) and the textures visualized in colors (B). The sample has a higher leucosome content than sample 1A and it also has larger grain size with the largest melanosome being over 3cm in size.

No drawing is included in Figure 18 as the sample 1C is quite homogeneously nebulitic. The sample is melanosome-dominated, with minor leucosome disrupting the continuity of the melanosome. The strain is still largely absent. The textures appear faintly directional horizontally in the Figure. This sample exhibits a homogenously mixed, nebulitic texture with fine-grained leucocratic material dispersed within a melanocratic matrix. The average grain size of sample 1C is small with large grains being a few millimeters in diameter.

Fig. 18: Sample Laassaniemi 1C.The sample shows no visible strain-related structures and contains only minor amounts of leucosome. The texture is nebulitic and equigranular with grain size being around 1 to 3 mm.

In sample 1D (Fig. 19) the structure is relatively leucosome-dominated, while the melanosome seems to surround the leucocratic areas. The rock is moderately directional horizontally in the figure and the textures are also elliptical parallel to the direction. The leucosome varies in color from white to beige. The flow structure seems to be present. The diameter of the grains in the sample ranges from 0.5 cm to around 2 cm.

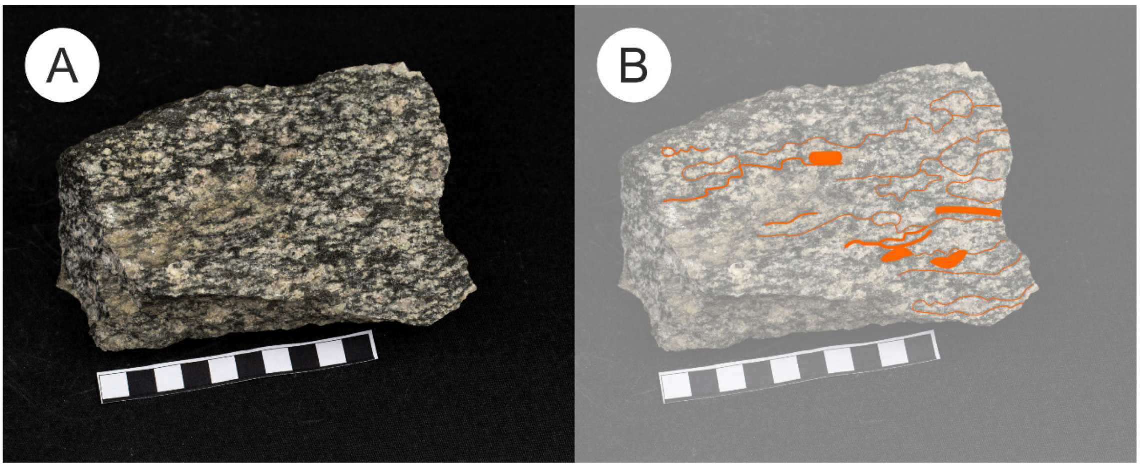

Fig. 19: Sample Laassaniemi 1D (A) and the general textures visualized (B). This sample shows strain textures with the grains being oriented. The leucosome and melanosome are also quite well separated with grain sizes being around 0.5 cm to 1.5 cm.

5.2.2 Laassaniemi 2

Sample 2A (Fig. 20) exhibits almost completely leucocratic textures with some small-scale melanosome patches. In addition, the sample contains some mint-colored stripes in the middle and an intact pyrite grain (circled in red on the bottom right of the sample). No apparent directionality is visible in the sample. The sample is almost completely composed of felsic leucosome. The few grains that the sample exhibits range from 1mm to 8mm in diameter.

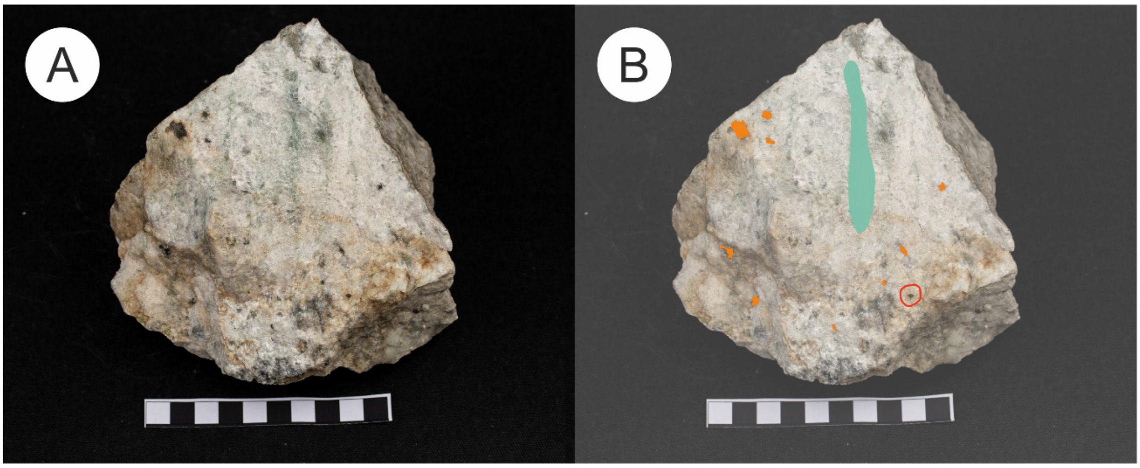

Fig. 20: Sample Laassaniemi 2A (A) and the structure visualized (B). This sample exhibits few grains of melanosome and is mostly composed of leucosome mass. The grains that are present remain quite euhedral and non-directional.

Laassaniemi 2B is largely dominated by homogenous melanosome (Fig. 21). Leucosome rafts are scattered around the rock sample and appear to be non-directional and randomly oriented.

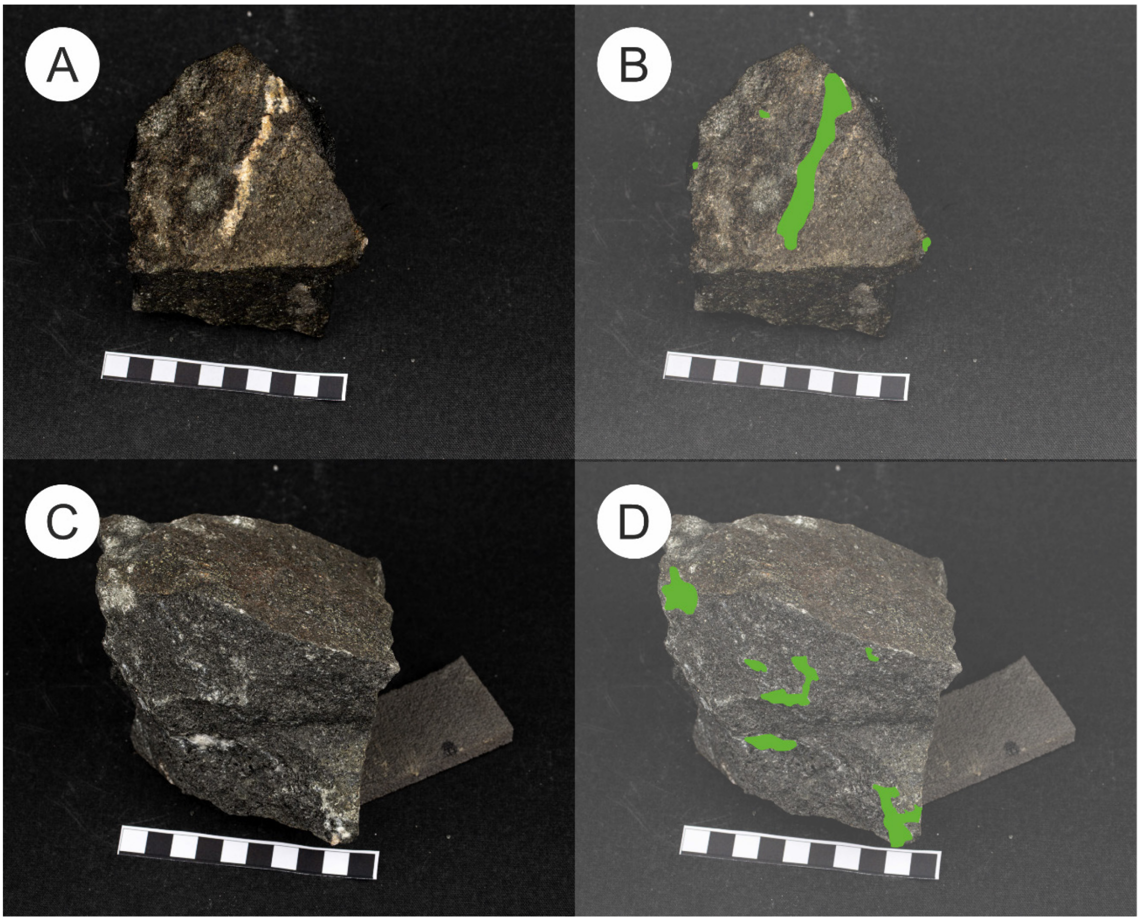

Fig. 21: Sample Laassaniemi 2B from two different surfaces (A and C) and their textures visualized in color (B and D). The sample exhibits a melanocratic texture with a well-defined leucocratic vein intruding the melanocratic mass. Some patches can also be seen in Figures C and D.

The sample 2C has an exceptionally heterogeneous structure (Fig. 22) and contains many leucocratic and melanocratic parts, while also exhibiting some areas where the distinction between melanosome and leucosome is difficult. The textures are heavily oriented, and the proportion of leucosome appears to be higher, around 50%.

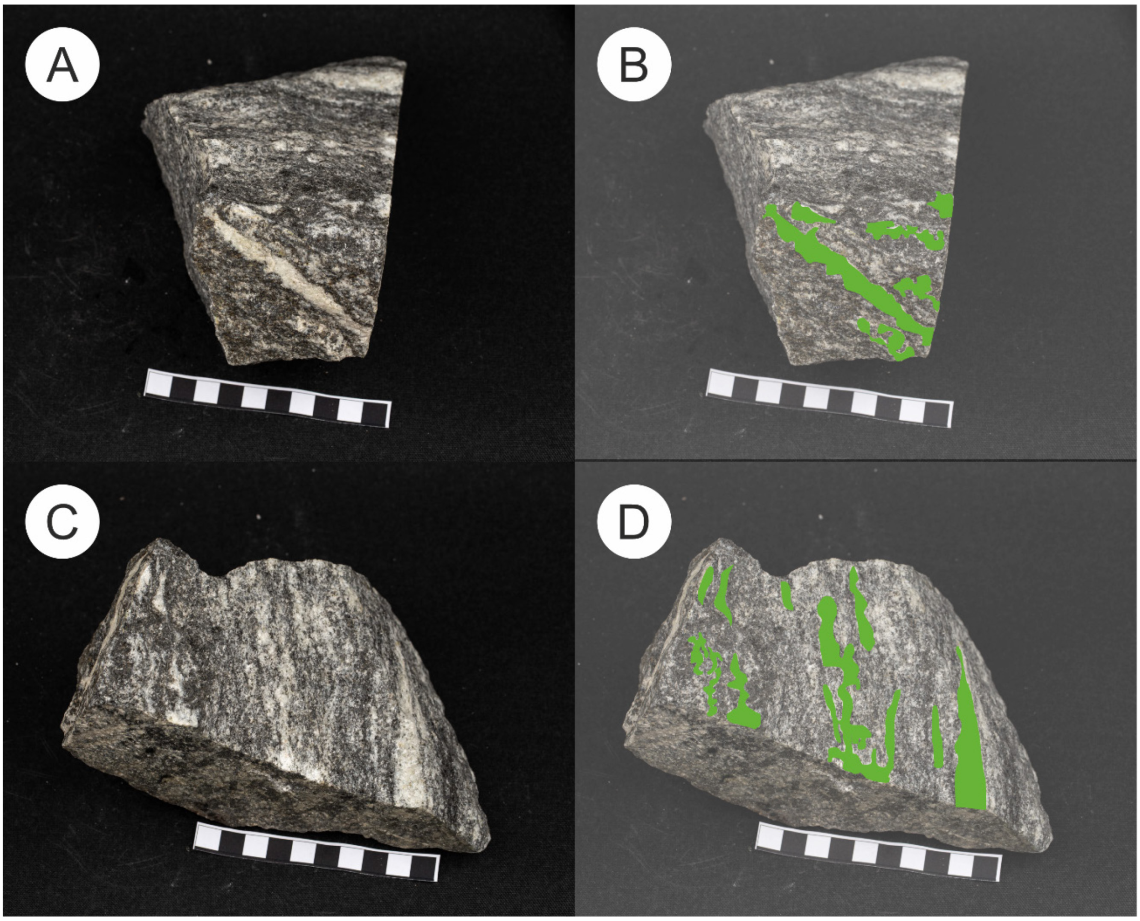

Fig. 22: Laassaniemi 2C from two different surfaces (A and C) and their textures shown in color (B and D). This very directional sample shows the flow structures of the melanosome-leucosome transition quite well.

5.2.3 Laassaniemi 3

Laassaniemi 3A, (Fig. 23), shows a distinct leucocratic vein cutting the melanocratic mass. Smaller felsic patches are absent from this sample, and the melanosome appears to be a film metatexite texturally. The leucosome fraction is quite low but evenly spread around the melanosome.

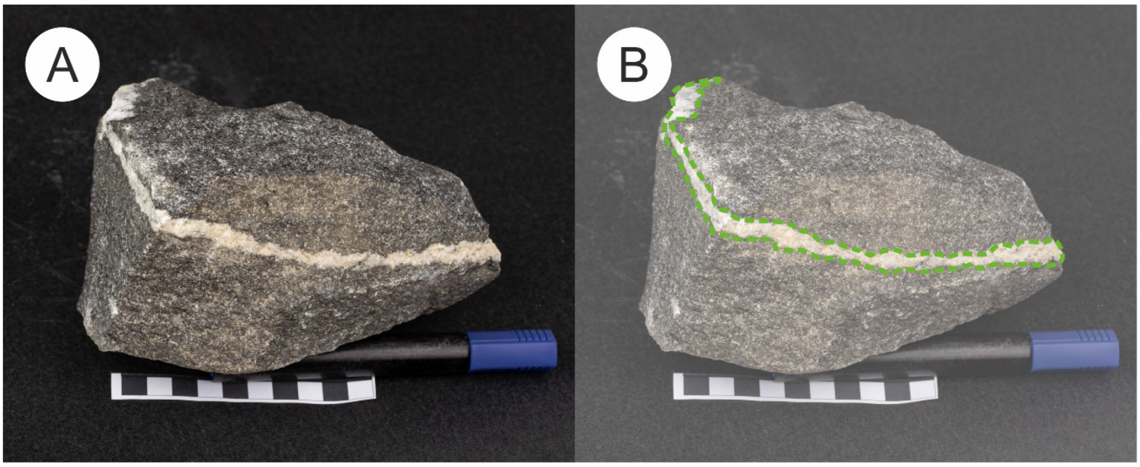

Fig. 23: Sample Laassaniemi 3A (A) and the textures visualized (B).

Laassaniemi 3B (fig. 24) is comparable to the sample 1B (Fig. 17) as it contains similar textures and patterns: Clearly separated leucosome, melanosome and neosome. While most of the material is separated into these three parts, none of them seem to be completely homogeneous and, for example the leucosome contains small patches of melanosome.

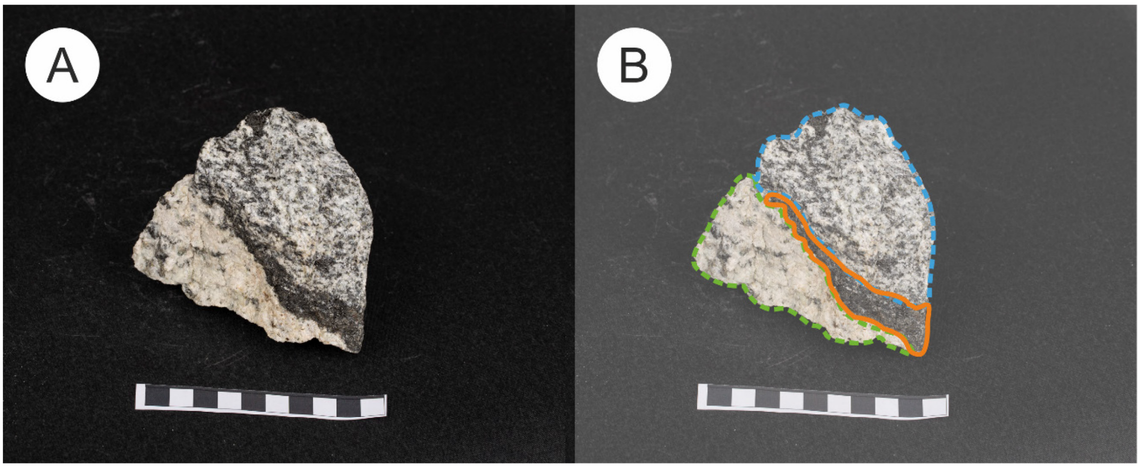

Fig. 24: Sample Laassaniemi 3B (A) and the textures visualized (B).

Laassaniemi 3C has distinctive patches of melanosome, which are large, around 5mm in diameter (Fig. 25). They are slightly oriented, but the directionality is hard to spot from singular melanosomes. The two images Figure 25 A and C show opposite sides of the rock sample. The leucosome fraction is high, but larger melanosome schlieren and rafts are still visible. The grain size varies from 0.5 cm to over 2 cm.

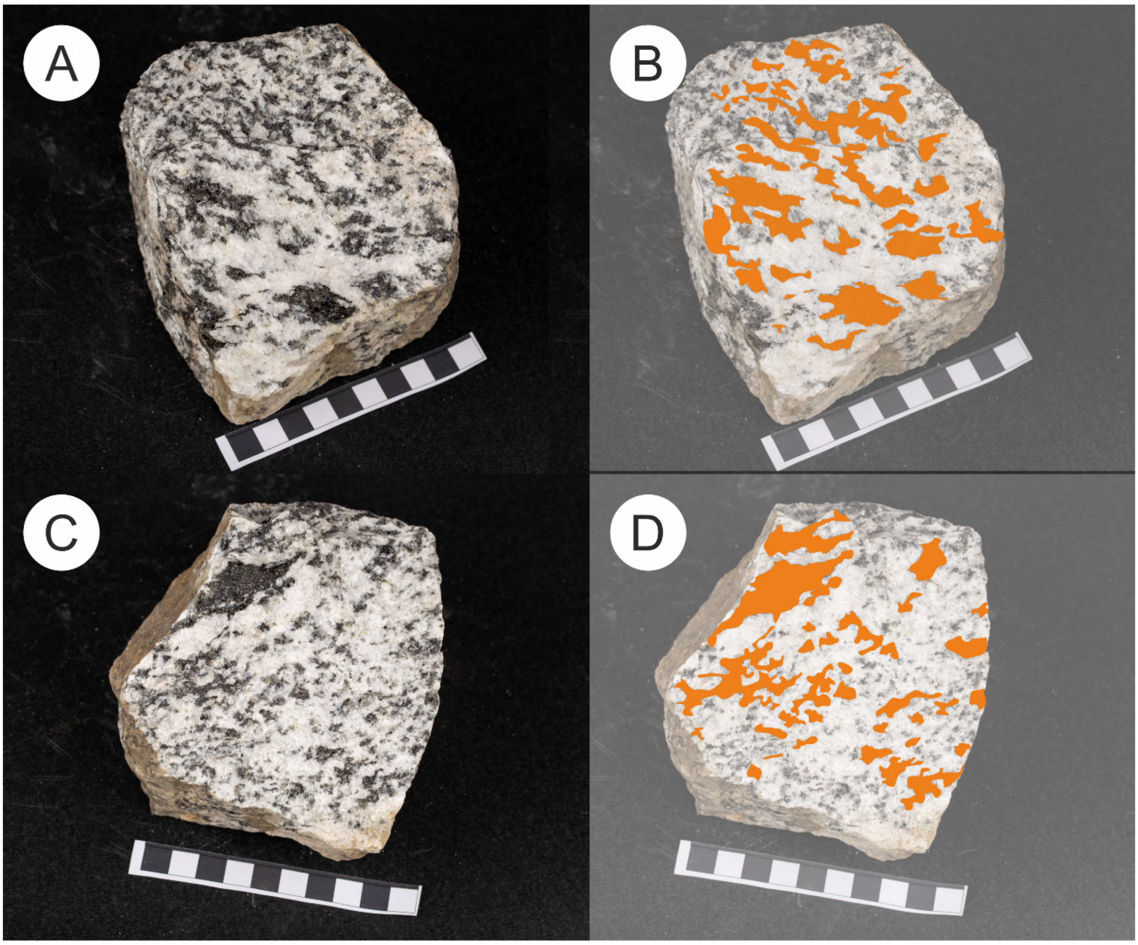

Fig. 25: Sample Laassaniemi 3C (A and C) and the melanocratic textures visualized in orange (B and D).

Laassaniemi sample 3D does not really have heterogenities (Fig. 26) and the ligher areas are mostly just post-formation scratches. The sample shows a quite nebulitic texture with sparce leucosome. The sample has visible grains but their size is less than 1 mm in diameter.

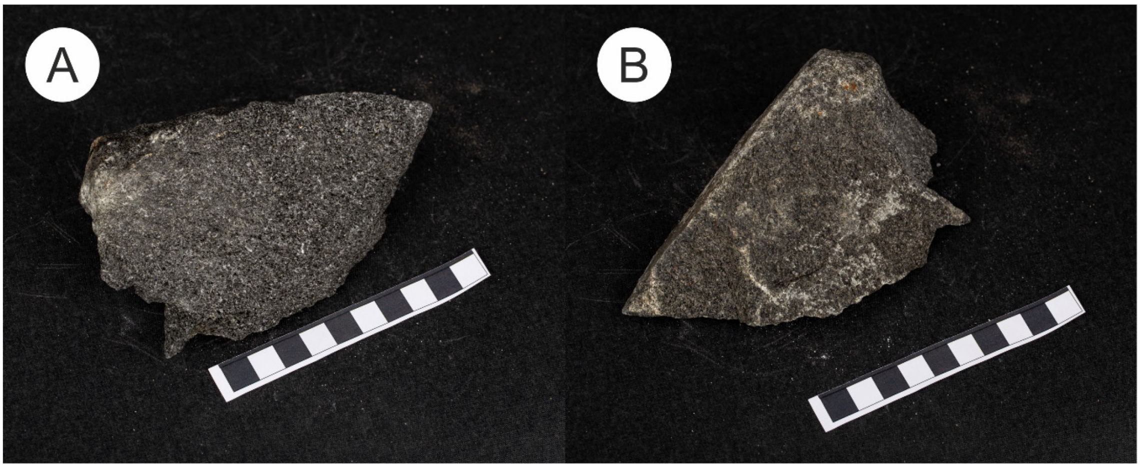

Fig. 26: Sample 3D from opposite surfaces. This sample has very homogenous melanocratic structure and a grain size of less than 1 mm.

5.3 Petrography and microscopy

The following pictures from thin sections contain a plain-polarized light (PPL) image and a cross-polarized light (XPL) image from the same position. Microscopically the granodiorite in the area is mostly granoblastic. This is due to the main mineral biotite (Bt) spreading evenly around the area. Other main minerals include oligoclase plagioclase (Pl), quartz (Qz), K-feldspar (Kfs) and epidote (Ep). In addition, some hornblende (Hbl) and alteration products of chlorite (chl) and carbonate (C). Accessory minerals comprise apatite (Ap), titanite(Ti), zircon (Zr) and occasionally magnetite (Mgn). The mineral assemblage has experienced epidote-amphibole facies conditions, where it has stabilized (Lehtovaara 1995).

5.3.1 Laassaniemi 1 thin section images

Sample 1A gets most of its dark colors from biotite and plagioclase, which are abundant in the sample (Fig. 27). The sample seems to be directional as the biotite grains are elongate. Some carbonatization can be seen in Figures 27 C and D at the edges of the K-feldspar. The sides of the image contain mortar-textured plagioclase.

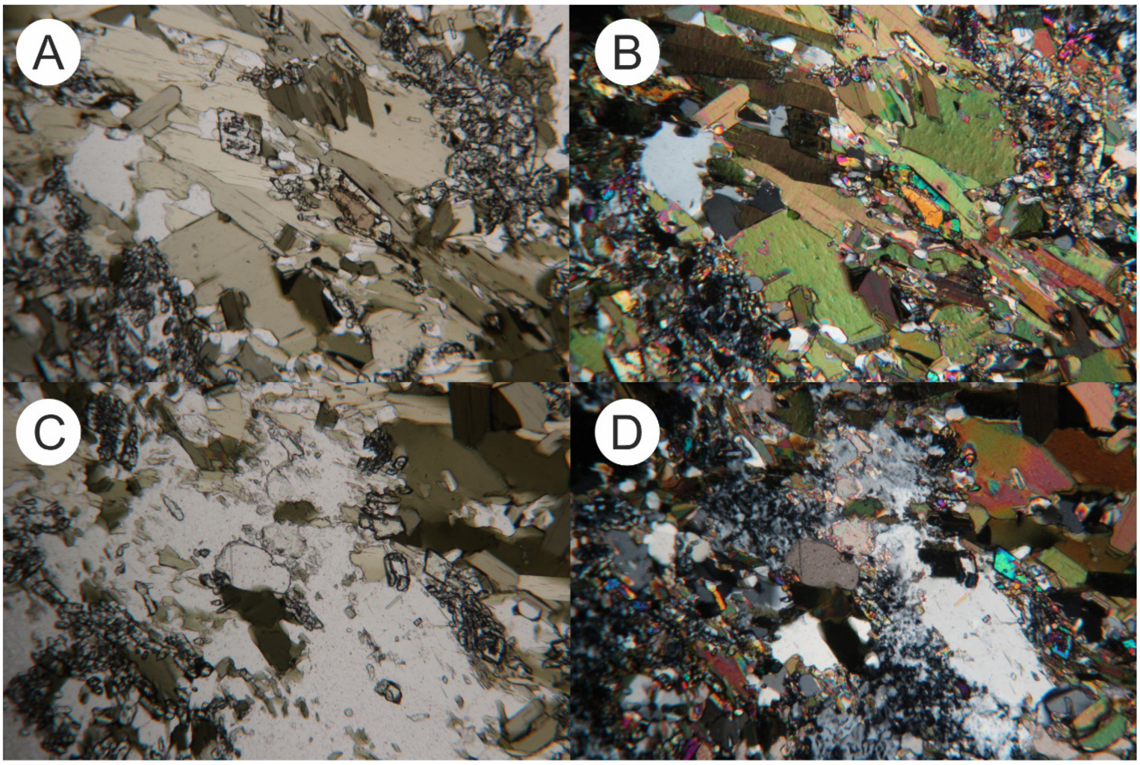

Fig. 27: Sample 1A thin section images. The image is around 3.2 x 2 mm in dimensions. This sample contains major Bt with recrystallized Qz and Pl. Pl is seen with a mortar texture in the bottom left corner of images B and D.

Sample 1B is considerably lighter than 1A in color and it also has high quartz content (Fig. 28 C) seen as a big off-white patch and as a mosaic black and white area (Fig. 28 D). The sample seems less directional compared to 1A, but it can also be due to the harder nature of quartz. The biotite grains in image C are still oval-shaped and directional. The sample 1B is quite equigranular. Some mortar-textured plagioclase can be seen in the matrix between the biotite grains on the right side of Figure 28 B and on top in 28 D.

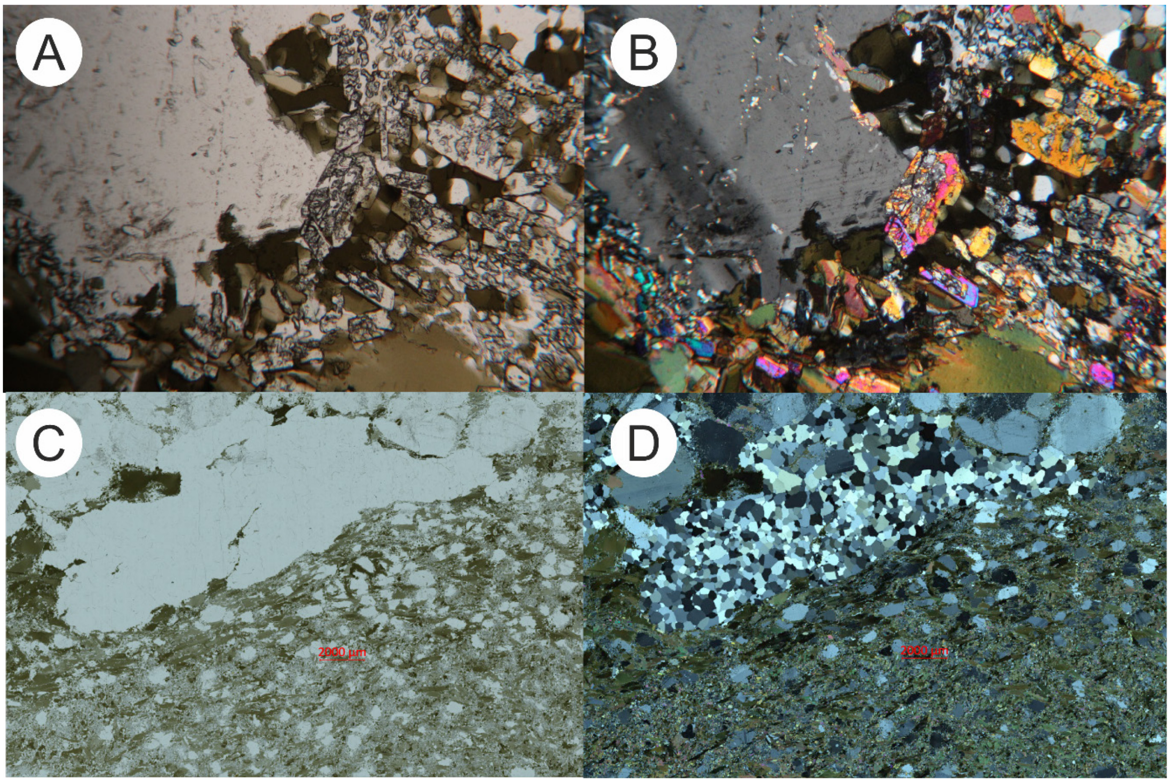

Fig. 28: Sample 1B thin section images. The dimensions of images A and B are around 3.2 x 2 mm. This sample is quite heterogenous as can be seen in figure 14. The quartz in the bottom half of images C and D is recrystallized to a mosaic pattern, and the biotite is heavily oriented around the quartz.

Sample 1C (Fig. 29) has similarities to both 1A (Fig. 27) and 1B (Fig. 28), being quite nebulitic structurally. The biotite grains are oval-shaped while the quartz and plagioclase appear to be quite round and undeformed. The biotite portion of the sample is slightly smaller than that of the lighter minerals’.

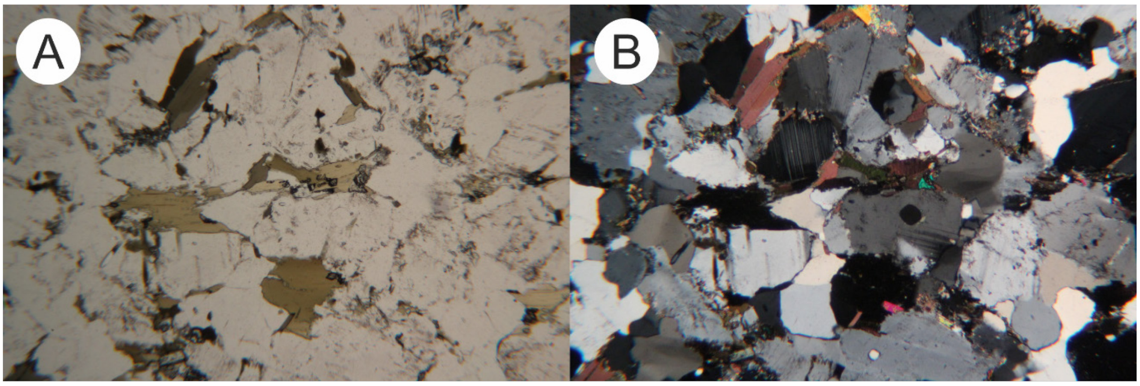

Fig. 29: Sample 1C thin section images. This sample exhibits nebulitic textures and the grains are subhedral. The recrystallized quartz exhibits mosaic texture in cross-polarized light (B). The dimensions of the images are around 3.2 x 2 mm.

Sample 1D has interesting but characteristic structures and alteration products. In Figures 30 A and B the general composition of the rock is shown, and in addition includes accessory allanite, which is shown in A and B above the scale as light brownish mass. Figure 30 C and D shows hornblende alteration to biotite, which is identifiable by the asymmetrical pleochroism in the bottom left of the image. In cross-polarized light (D) it appears as crack-like texture, where the cracks show high interference colors. The sample also has common quartz and mortar plagioclase in images A and B, in the upper right corner. The grain size appears to be around 1 mm in quartz and less than 1 mm in darker minerals such as biotite.

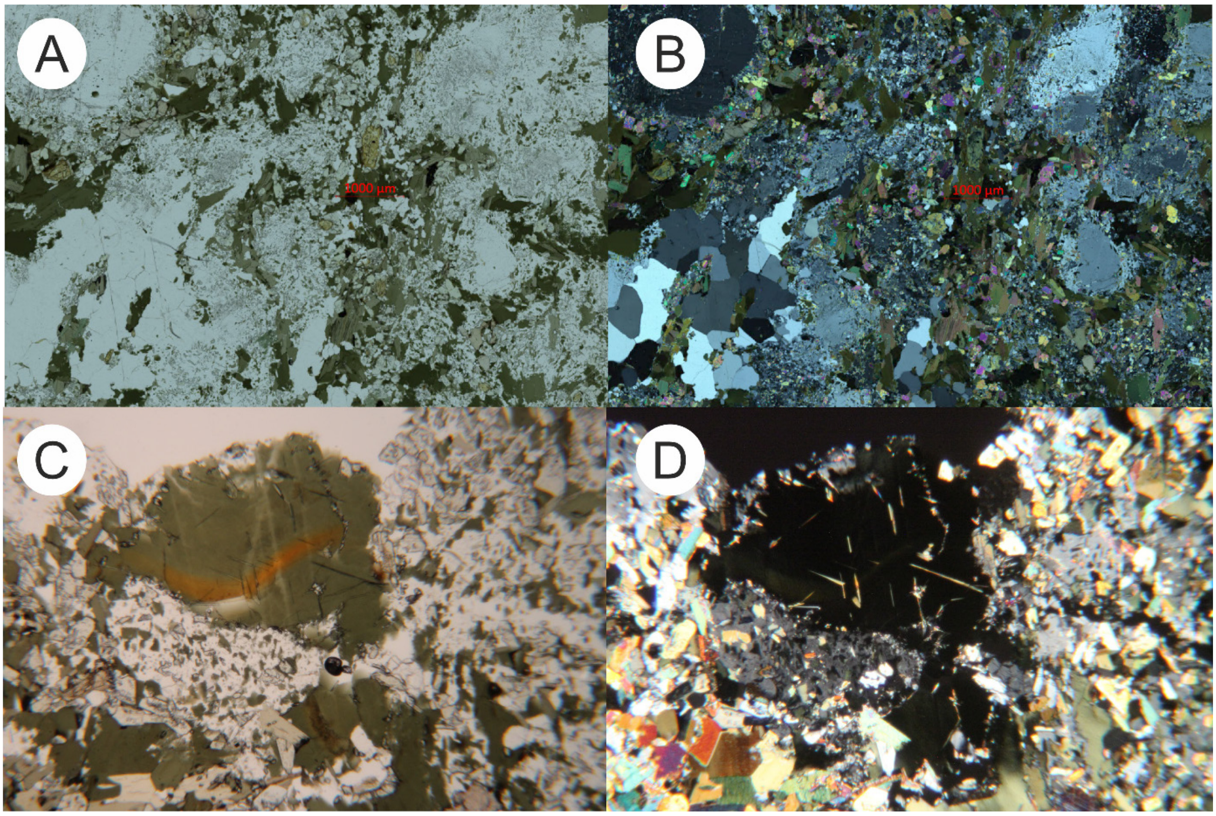

Fig. 30: Sample 1D thin section images. This sample contains abundant Bt and distinct differentiation patterns in the Bt. The dimensions of images C-D are 1.2 x 0.8 mm.

5.3.2 Laassaniemi 2 thin section images

Laassaniemi 2A (Fig. 31) has abundant plagioclase and quartz which is the reason for its light color. Its inequigranular structure shows larger K-feldspar grains and smaller quartz grains in comparison. Some chlorite can be found in the bottom right corner of image B. The cross-twinning of K-feldspar can be seen in image D in a considerably large grain compared to the rest of the rock mass. The average grain size in the sample appears to be larger compared to the other samples. The sample does not have visible darker minerals in sample images.

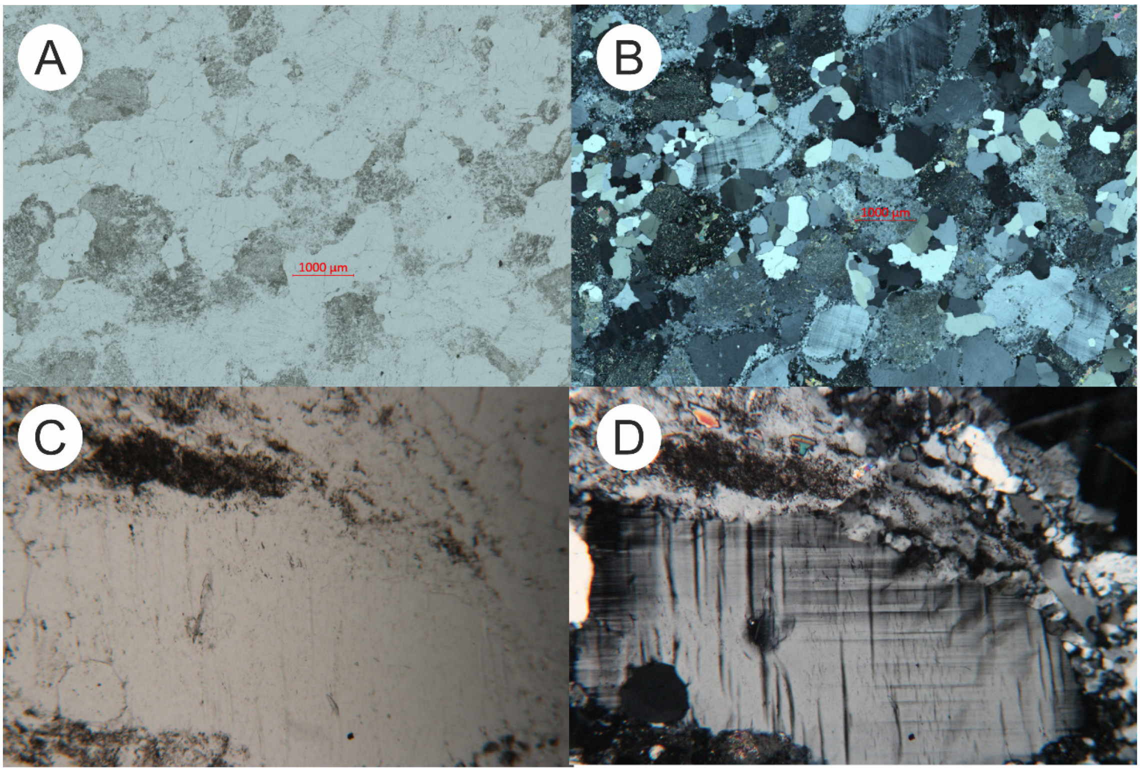

Fig. 31: Sample 2A thin section images consisting mainly of recrystallized Qz, Kfs and Pl. The dimensions of the images C-D are 3.2 x 2 mm. The grain sizes for Qz are smaller at around 0.5 mm and the Kfs grain seen in image D is over 3 mm in diameter.

Sample 2B is of a darker color, which is caused by the higher content of biotite. The upper image is taken from near the white vein (Fig. 32 A and B) explaining the high plagioclase and quartz content. Figure 32 C and D show quite unoriented biotite grains and chlorite. The biotite grains seem to be larger in comparison to the other darker grains in Figure 32C but also much smaller in Figure 32A compared to the plagioclase.

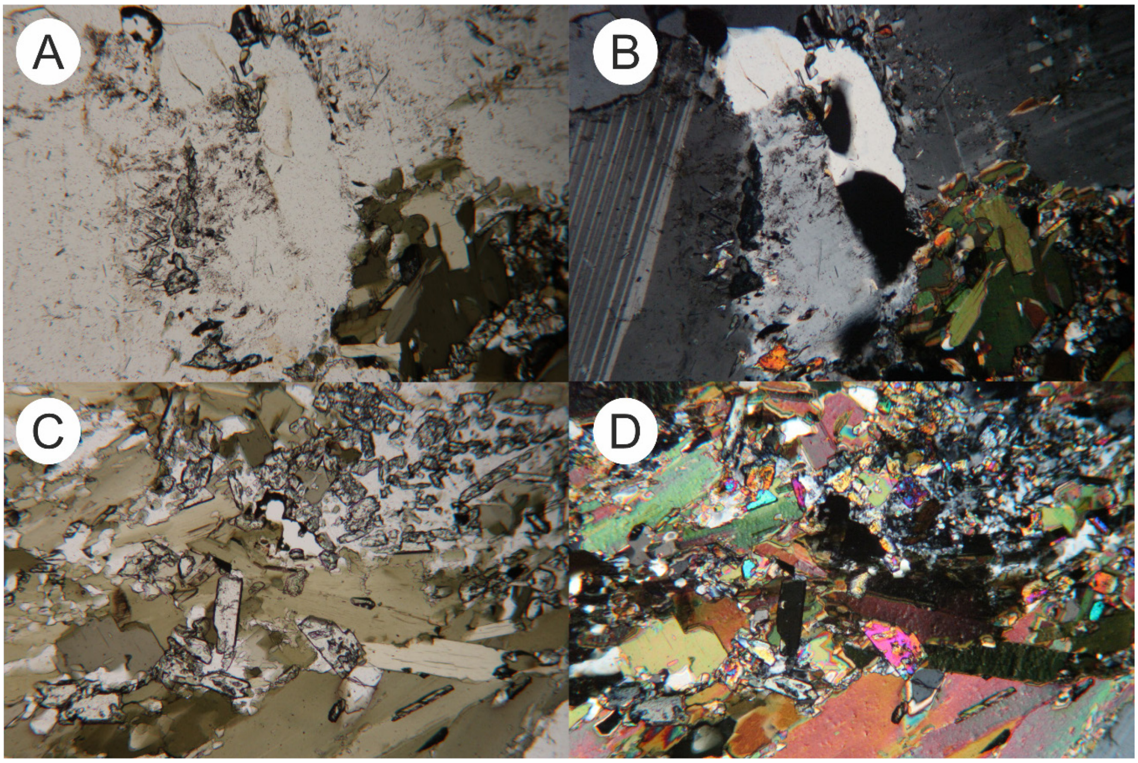

Fig. 32: Sample 2B thin section images. The dimensions of the images are around 3.2 x 2 mm. This sample is mostly biotitic except for the leucocratic vein (A and B, Fig. 18). The grain size ranges from 0.3 mm to around 1 mm for Bt and over 1 mm for Pl. The mortar Pl is under 0.1 mm in grain size (C and D).

The sample 2C thin section, seen in Figure 33, reflects its directional and relatively high leucosome content. The melanosome appears to be in tiny grains of biotite, while leucosome is presented as larger grains of quartz and plagioclase. The orientation of the biotite minerals seems to follow the leucosome borders, and the relative crystallization ages seem to be older for darker minerals such as biotite.

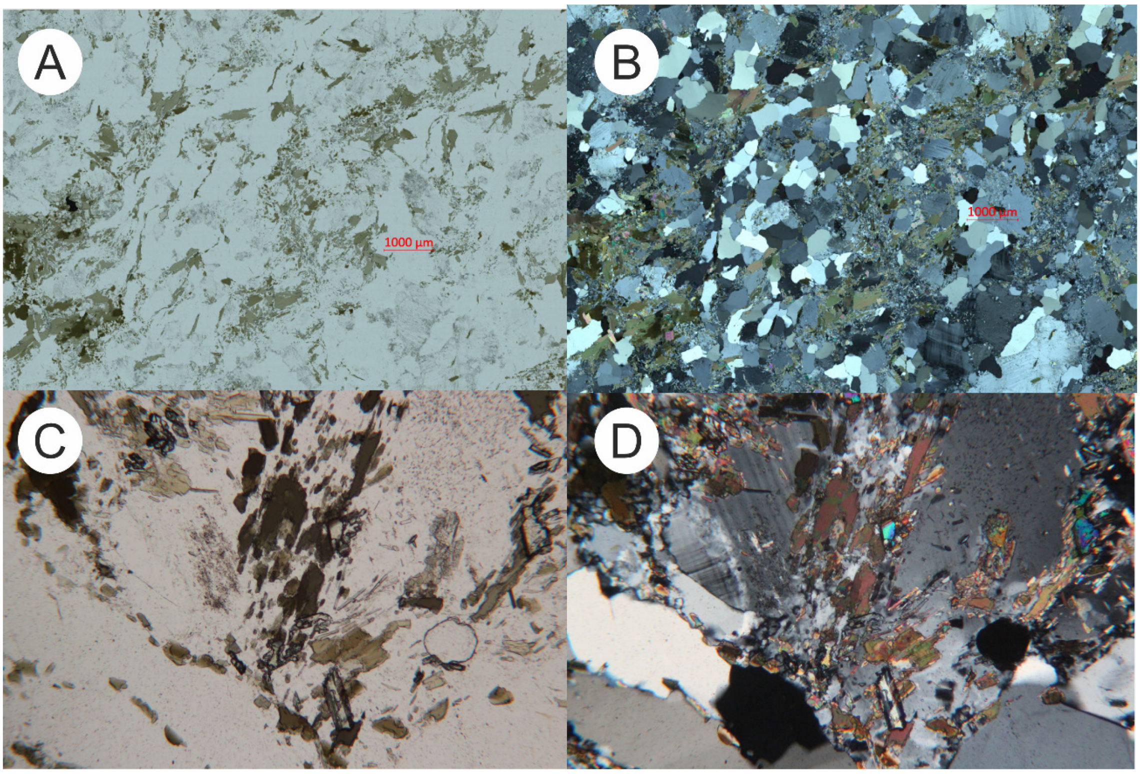

Fig. 33: Sample 2C thin section images. Image C-D dimensions are around 3.2 x 2 mm. This sample contains larger Qz and Pl grains with considerably smaller Bt grains, which are more elongated structurally compared to the rest of the sample. The grain size of Bt is from 0.1mm to about 0.5 mm while the bigger quartz and plagioclase grains range from 0.7 mm to over 2 mm.

5.3.3 Laassaniemi 3 thin section images

Laassaniemi 3A sample has a nebulitic base structure but there is a lighter vein running through the sample, which can be seen in Figure 34A and B. The lighter vein contains mostly quartz and K-feldspar. The darker minerals seem to have surrounded the lighter ones as seen in images C-D. The center of these images also exhibit carbonate in small amounts.

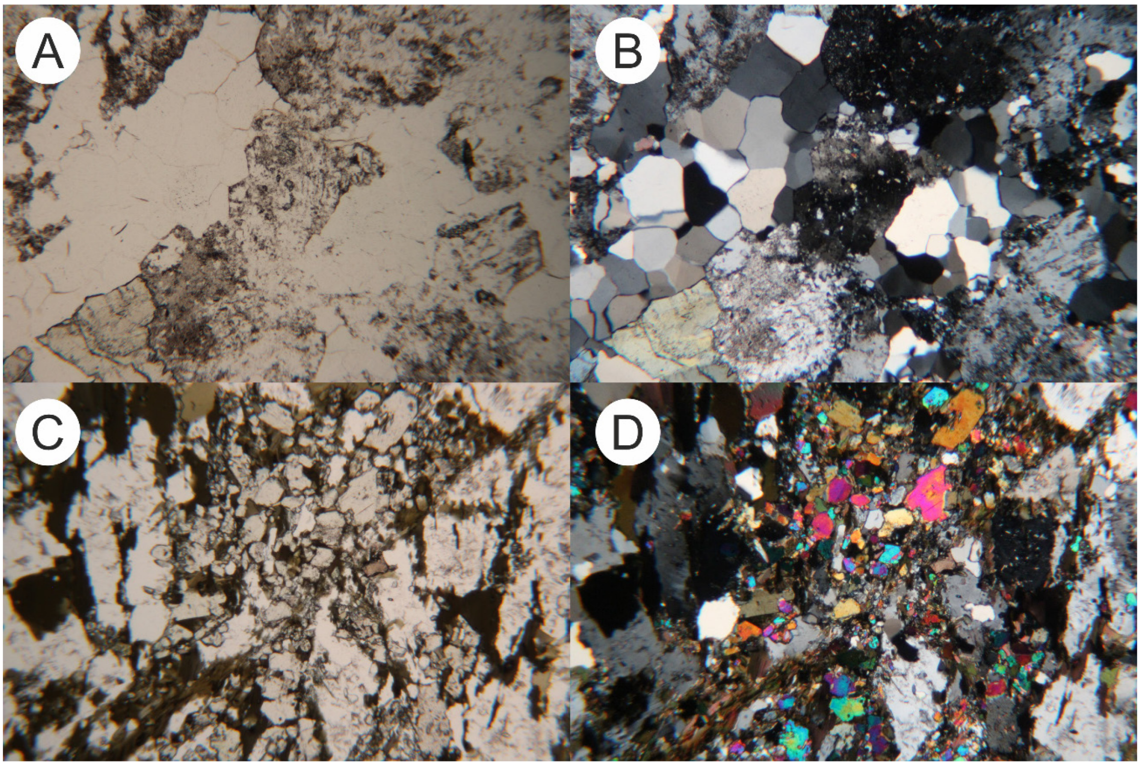

Fig. 34: Sample 3A thin section images. Images A and B dimensions 1.2 x 0.8 mm. C & D around 3.2 x 2 mm. Images A and B are mainly composed of Kfs and recrystallized Qz. Images C and D have Kfs crystals that are surrounded by a Bt matrix, and in the middle of the image is also some carbonate.

Sample 3B (Fig. 35) exhibits considerably larger grains of quartz, K-feldspar and plagioclase than previous samples. Biotite grains are also larger in comparison. No apparent orientation can be seen in the thin section images. Figures 35E and F show microstructures starting to form inside larger grains indicating recrystallization.

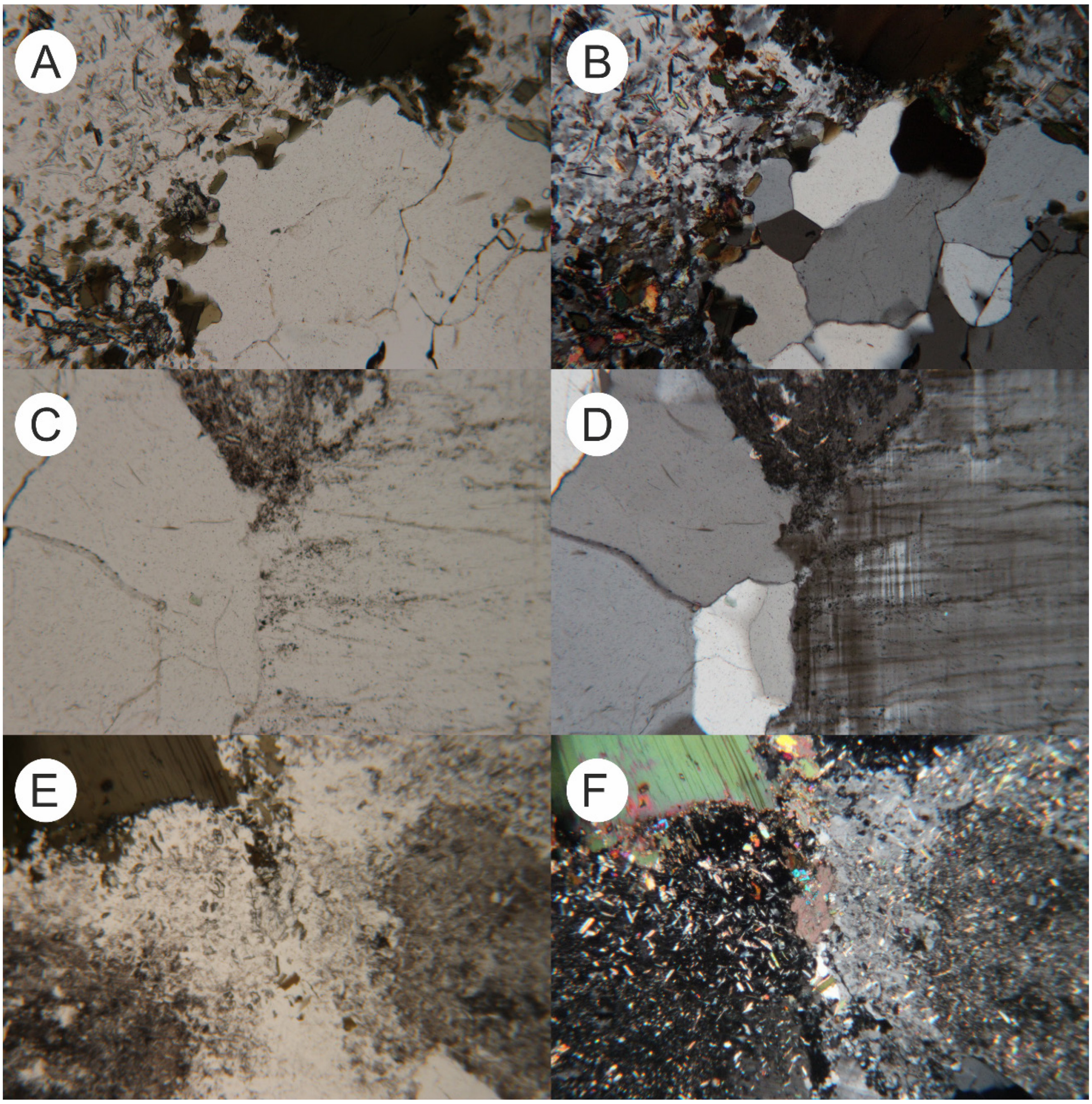

Fig. 35: Sample 3B thin section images. Images A-D dimensions are about 3.2 x 2 mm, while images E-F are around 1.2 x 0.8 mm. This sample has more light-colored minerals which can be seen in images A-D. Images E-F exhibit granular Kfs with a bigger Bt grain in the bottom right corner of the image.

Sample 3C (Fig. 36) is dominated by light minerals, with some bigger dark patches of biotite and chlorite in between. Figures 36A and B show altered mineral grain edges. It appears that the edges of these grains have been melted and mixed together. In Figure 36 C and D some allanite is also present at the center of the images C and D. The rest of these images are dominated by quartz and K-feldspar.

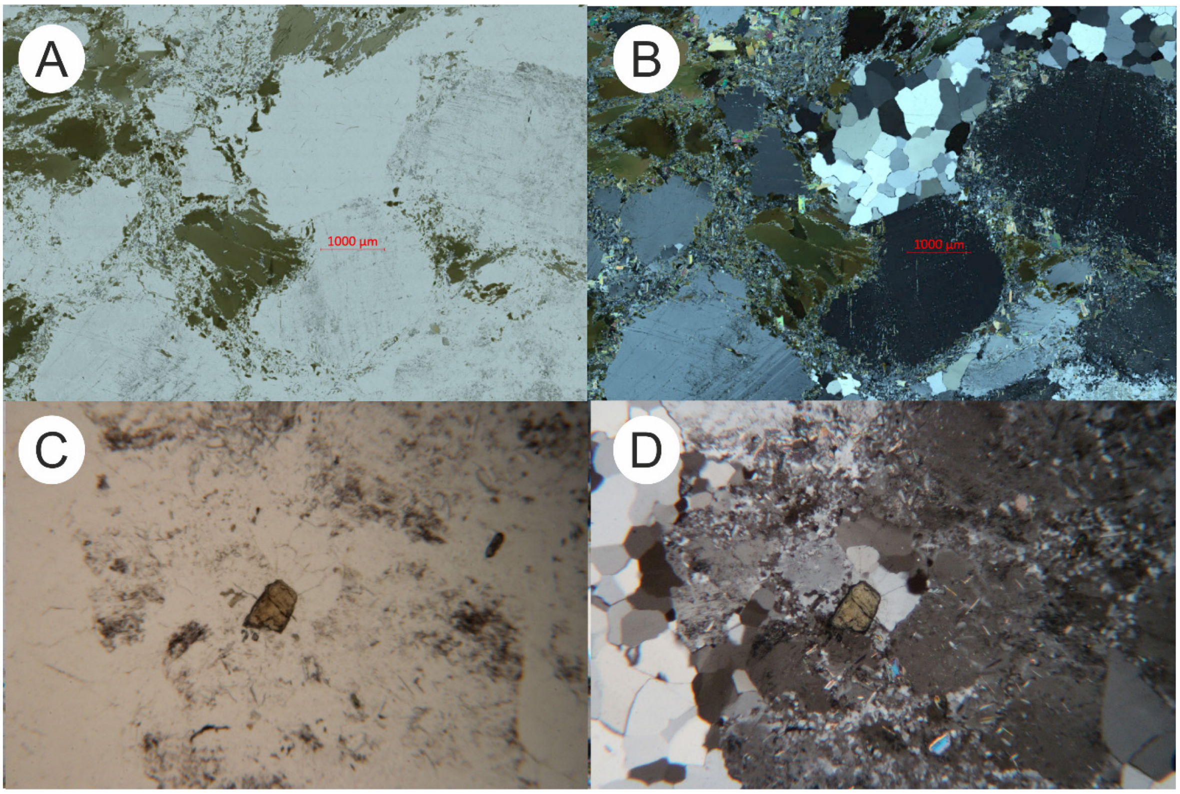

Fig. 36: Sample 3C thin section images. The thin section includes quartz and plagioclase as a white mass and some biotite in Figure 33A. This sample is quite similar to 3B in composition, and the relative amounts of light minerals compared to biotite are quite the same.

Sample 3D has small but quite inequigranular grains and a nebulitic texture, explaining the very even amount of darker and lighter minerals, as can be seen in Figure 37 A and 37 C. The texture seems to be only slightly oriented. The grain size in this sample is very small, and only under 0.5 mm grains can be seen in images A and B. Images C and D contain only a few large grains which are quite elongated structurally.

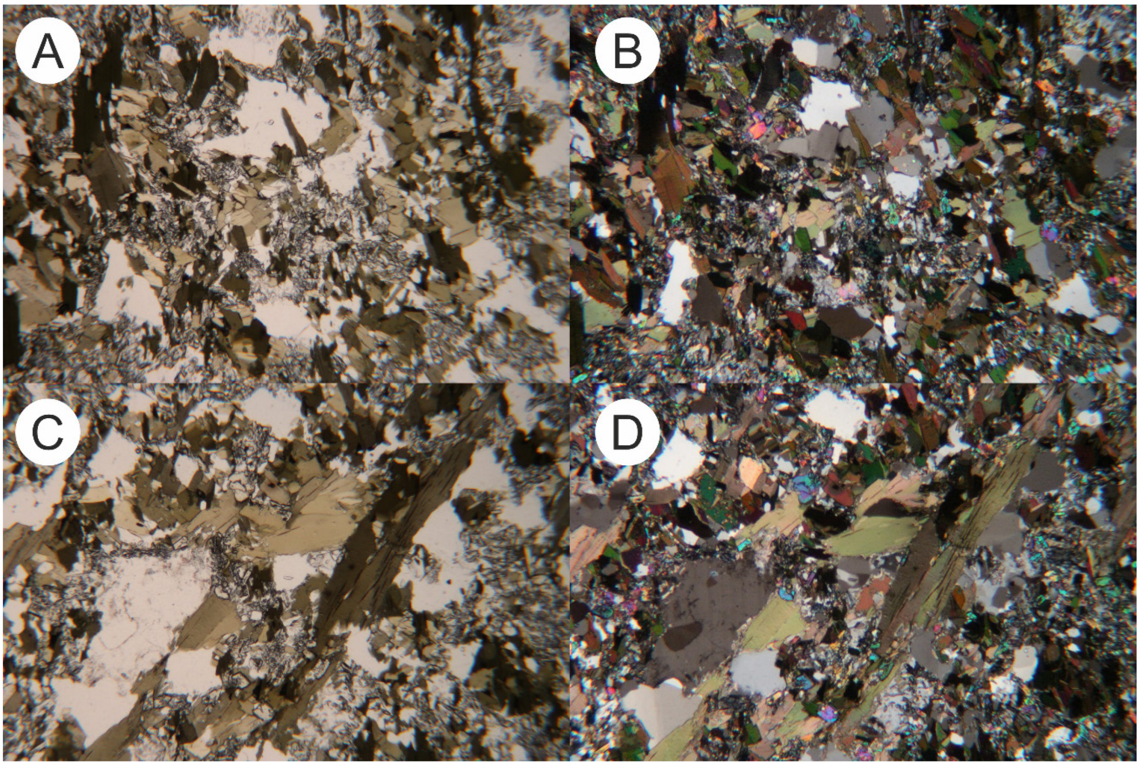

Fig. 37: Sample 3D thin section images. Image dimensions are about 3.2 x 2 mm. This sample is very biotite-rich, and the matrix contains mortar plagioclase and other accessory minerals.

6 Discussion

Structural observations from the Laassaniemi roadcut indicate that a substantial proportion of the protolith has been partially melted and mobilized during anatectic flow (Appendices A and B). Only a few larger residual blocks of protolith remain preserved within the outcrop. The presence of boudinage structures, together with a pronounced increase in melt fraction north of the boudin neck, suggests concentration of the leucocratic material in structurally controlled low-pressure domains. This spatial distribution reflects transfer through the boudin neck from the more leucocratic northern domain. The occurrence of leucocratic material within the melanocratic amphibolite protolith further supports the interpretation that infiltration preferentially occurred along pressure-shadow zones associated with boudinage deformation (Fig. 11)

The Laassaniemi outcrop displays well-developed metatexite–diatexite transition structures, where diatexitic material locally occurs as thin veins within metatexite domains (Fig. 11). These relationships suggest internal melt redistribution within a partially molten framework rather than large-scale external intrusion. According to Halla (2020), migmatites in the Rommaeno TTG terrain were generated by *in-situ* or *in-source* melting, and metatexite–diatexite transitions are widespread within these Archean migmatitic domains. The structural features observed at Laassaniemi are in line with this regional pattern.

Overall, the melanosome is predominantly biotite-rich in composition, except for the minor hornblende (e.g. Fig. 30 C and D). This suggests that melting involved biotite-consuming reactions during anatexis rather than simple melting of individual mineral phases. The felsic domains are dominated by quartz and K-feldspar, which crystallised from the melt and commonly display little preferred orientation. Biotite locally occurs as irregular patches and discontinuous aggregates along grain boundaries, possibly occupying sites created during melt segregation (Fig. 36). Such distributions may mimic flow patterns, and oval-shaped biotite aggregates could represent residual material redistributed during crystallisation of the felsic phases.

6.1 Stages of melting in Laassaniemi

6.1.1 Incipient melting

The protolith of the Laassaniemi migmatites is interpreted to have been an amphibolite (Halla 2020). This interpretation is supported by the preservation of dark melanocratic domains within the outcrop and by the observed mineralogical characteristics (Appendix A, Figures 16, 21, 23 and 26).

The earliest evidence of melting at Laassaniemi is represented by randomly oriented leucosome bodies enclosed within a dominant paleosome framework, together with subtle leucosome films developed along grain boundaries (Figures 16, 21 and 23). These features support the interpretation that low melt fractions remained largely in situ and did not yet form interconnected networks.

Thin-section observations of the corresponding samples show a predominance of darker minerals (Bt, Pl), while incipient melting is reflected in the development of mortar-textured plagioclase and the presence of biotite-rich selvedges along grain boundaries (Fig. 36). Quartz recrystallisation structures observed within lighter leucocratic veins are in agreement with melt formation and subsequent segregation during *in-source* melting (Fig. 23).

6.1.2 Transitional melanosome-leucosome migmatization

With increasing melt fraction, melt distribution becomes progressively heterogeneous, resulting in the development of patch migmatitic textures. Such textures occur in the roadcut and in patch migmatites (Figures 18 and 22).

Vein migmatites develop as leucosome accumulates in structurally controlled low-pressure sites, such as pressure shadows. These features do not necessarily represent a separate melting phase but rather local melt redistribution within the partially molten framework. Ptygmatic folding of leucocratic veins is observed adjacent to the boudinage structure in the roadcut, while vein structures without ptygmatic folding also occur (Figures 21 and 23).

A boudin neck is present in the central part of the roadcut. Towards the north of the neck, the rock becomes progressively more leucocratic. Adjacent to the boudin, schlieric textures developed within a nebulitic framework are observed. This spatial distribution is consistent with melt migration through the boudin neck towards the south (Appendix A).

Transitional melting is also reflected in thin-section textures, where an increased proportion of subhedral and anhedral grains is observed. Darker minerals commonly appear elongated and are aligned along grain boundaries. The samples display more developed nebulitic textures, characterised by increasingly even proportions of light and dark mineral phases.

6.1.3 Diatexite migmatization

As melt fraction increases, melanosome rafts become dispersed within a leucosome-dominated matrix (Fig. 12). At this stage, the rock framework has largely lost its structural cohesion. In the northern part of the roadcut, melanosome is preserved only as isolated rafts or nebulitic domains. The alignment of these rafts indicates syn-anatectic deformation and melt movement within the partially molten system.

The most diatexitic areas at Laassaniemi are characterized by leucosome-dominated textures and quartz-rich compositions, reflecting high melt fractions. Comparable textural and compositional features are observed in the most leucocratic samples (Figures 17, 24 and 25). Thin sections of the most leucocratic domains are dominated by quartz and feldspar, while biotite is concentrated along quartz grain boundaries. In these samples, biotite commonly occurs as fragmented or discontinuous aggregates and locally forms selvedge-like structures surrounding quartz grains.

Near-homogeneous leucosome domains are characterized by a mineral assemblage dominated by plagioclase, quartz and K-feldspar and by the absence of a clear directional fabric. Thin-section observations show only minor amounts of mafic minerals, and the feldspar and quartz grains commonly display euhedral to subhedral crystal forms (2A). The lack of foliation and the predominance of equant felsic minerals are compatible with crystallization from a melt-dominated system, where melt fraction locally exceeded the solid-to-liquid transition and deformation was limited during final crystallization.

6.2 Migmatite genesis interpretation

The Archean migmatites at Laassaniemi occur within a basement domain that is structurally overlain by the Caledonian orogen in the north and north-west (Fig. 7). The lateral extent of the migmatitic domain towards the south, east and west remains poorly constrained; however, similarly aged TTG rocks are documented in northern Sweden and may extend over several hundred kilometers along a SW–NE trend.

The Laassaniemi outcrop likely represents part of a broader metatexite–diatexite transition zone. This interpretation is based on the systematic variation in melt fraction and textural development observed across the outcrop, while adjacent rocks to the south lack clear evidence of partial melting. The overall size and continuity of this transition zone cannot be determined from the present dataset and would require investigation across a wider regional framework.

Although the crystallisation age of the host TTG rocks is constrained, the timing of migmatization itself remains unconstrained. The migmatization may have occurred shortly after TTG emplacement as part of a prolonged high-temperature evolution of the crust, or alternatively during a later thermal overprint. Comparable migmatitic textures are documented near Lake Inari, suggesting broadly similar metamorphic and melting conditions across the wider Rommaeno TTG terrain. This regional similarity supports the interpretation that migmatization reflects large-scale crustal reworking rather than a strictly localised phenomenon.

The Caledonian orogeny is unlikely to have played a significant role in the genesis of these migmatites. A clear structural and stratigraphic discontinuity separates the younger Caledonian units from the underlying Archean basement (Lehtovaara 1995), and no direct structural overprinting of Caledonian deformation is observed within the migmatitic domains. These relationships indicate that migmatization predates Caledonian tectonism and is more plausibly related to Archean crustal processes.

A broader regional dataset would be required to fully constrain the extent and nature of migmatization within the Rommaeno Complex. Halla (2020) documents extensive and laterally continuous metatexite–diatexite transitions within TTG terrains of Arctic Fennoscandia, suggesting that similar transition zones may be widespread in the region. The Laassaniemi outcrop may therefore represent one example of a more regionally developed migmatitic system.

7 Conclusions

The Kilpisjärvi migmatites represent a metatexite-diatexite transition structure that has most likely formed from a basaltic protolith. It formed through *in situ* and *in-source* partial melting. The area exhibits various metatexite and diatexite textures and no single migmatite type dominates the area. The roadcut from the Laassaniemi area shows a boudinage structure with amphibolite transitioning into nebulitic migmatite. Leucosome injection into the metatexite has produced a central film migmatite texture. This metatexite-diatexite transitioning seems to be common around Kilpisjärvi area and it likely extends regionally as a structurally continuous zone.

The studied samples are mineralogically similar but display a wide range of textures. Melt fraction varies widely, ranging from nearly unmelted to melt-dominated samples. The contacts between the melanosome and leucosome vary with some sharp contacts and other sections showing gradual transitions from pure leucosome to pure melanosome. Although the precise structural position of each sample cannot be determined, their characteristics correspond closely to the outcrops observed at Laassaniemi.

Thin sections show decreasing plagioclase and biotite content as melt fraction increases. Samples showing intermediate degrees of melting contain biotite selvedges surrounding residual biotite grains. With progressive melting, the biotite grains disappear, leaving only the selvedges between quartz and K-feldspar.

More study is required in the surrounding areas to better understand the linkage of the migmatites with the nearby geology. Geological information from the Swedish and Norwegian side is also important in determining the continuum of the complex. In addtiton, the possible linkage of Kilpisjärvi migmatites with Lake Inari migmatites could be studied.

Acknowledgements

I would like to thank my supervisors Esa Heilimo and Jaana Halla for continued support in this thesis. I want to thank the familiar faces of the Geohouse computer room for raising my spirits during the master thesis process. Additionally, thank you to Mari Nurmi and Hannu Nurmi for reviewing my thesis despite the lack of background in geological studies.

References

Bergman, S. (2018). *Geology of the Northern Norrbotten ore province, northern Sweden*, Geological Survey of Sweden, Uppsala, Rapporter och meddelanden 141: 64p.

Brown, M. (1973). The definition of metatexis and diatexis. *Geological Magazine* 110: 195–199. 10.1016/S0016-7878(73)80021-5

Halla, J. (2020). The TTG-amphibolite terrains of Arctic Fennoscandia: infinite networks of amphibolite metatexite-diatexite transitions. *Frontiers in Earth Science* 8: 252, 14 p. https://doi.org/10.3389/feart.2020.00252

Halla, J., Joshi, K. B., Luttinen, A., Heilimo, E., & Kurhila, M. (2024). On the origin of Archaean TTGs by migmatization of mantle plume-related metabasalts: Insights from the Lake Inari terrain, Arctic Fennoscandia. *Precambrian Research 407:* 18 p. https://doi.org/10.1016/j.precamres.2024.107407

Holness, M. B. & Watt, G. R. (2002). The aureole of the Traigh Bhàn na Sgùrra Sill, Isle of Mull: reaction-driven micro-cracking during pyrometamorphism. *Journal of Petrology 43*:3 511–534. https://doi.org/10.1093/petrology/43.3.511

Idman, H. (1988). Geological Map of Finland. Pre-Quaternary Rocks. Sheet 1832-Ropi, *Geological Survey of Finland* 2p.

Karinen T., Lepistö S., Konnunaho J., Lauri L., Manninen T. & Huhma H. 2015. Yksikkökuvausraportti Enontekiö, käsivarsi. *Geologian tutkimuskeskus Rovaniemi* 66/2015: 39 p. https://tupa.gtk.fi/raportti/arkisto/66_2015.pdf

Konnunaho, J., Halkoaho, T., Hanski, E. & Törmänen, T. (2015). Komatiite-Hosted Ni-Cu-PGE Deposits in Finland. *In mineral deposits of Finland Elsevier* 38 p. https://doi.org/10.1016/B978-0-12-410438-9.00004-2.

Konnunaho, J. (2018). Geological unit report: Sarvisoaivi mafic-ultramafic volcanic rock. *Geologinen tutkimuskeskus,* 3p.

Lehtovaara, J. J. (1995). Geological Map of Finland. Pre-Quarternary rocks of the Kilpisjärvi and Halti map-sheet areas. Sheets 1823 and 1842 *Geological Survey of Finland.* 66 p.

Maxeiner, R. O., Ashton, K., Card, C. D., Morelli, R. M., & Knox, B. (2017). A Field Guide to Naming Migmatites and Their Textures, with Saskatchewan Examples. Government of Saskatchewan, Miscellaneous Report 2017-4.2,. Regina, SK: *Saskatchewan Ministry of Economy*. 20 p.

Mehnert, K. R. (1968). Migmatites and the origin of granitic rocks. *Megascopic structures of migmatite*, 7–42.

Mindat web page: https://www.mindat.org/photo-899514.html (page visited 21.3.2025 14:09)

Riis, F. (1996). Quantification of Cenozoic vertical movements of Scandinavia by correlation of morphological surfaces with offshore data. *Global and Planetary Change 12:*1-4, 331–357. https://doi.org/10.1016/0921-8181(95)00027-5

Sawyer, E. W. (2008). Atlas of migmatites*. The Canadian Mineralogist Special Publishment Vol. 9.*

Sederholm, J.J. (1907). Om granit och gneiss, deras uppkomst och inbördes förhållanden. *Bulletin de la Commission Géologique de Finlande* No. 23: 1–80. [In Swedish]

Zhang, J., Liu, W., Yakymchuk, C., Sa, R., Zeng, Z., Ding, R., Tang, G., Liu, H., Xu, Q., & Wang, Y. (2019). Partial Melting and Crustal Deformation during the Early Paleozoic Wuyi–Yunkai Orogeny: Insights from Zircon U-Pb Geochronology and Structural Analysis of the Fuhuling

Migmatites in the Yunkai Region, South China. *Minerals*: *9*(10), 621.
https://doi.org/10.3390/min9100621

Appendices

Appendix A: A stitched together image of the Laassaniemi roadcut on the eastern side of the road. The image is directioned north to south.

Appendix B: Laassaniemi roadcut textures drawn.